Published version : doi: 10.1016/j.addr.2021.113826

The importance of pre-formulation studies and of 3D-printed nasal casts in the success of a pharmaceutical product intended for nose-to-brain delivery

Laura Deruyver [a†], Clément Rigaut [b†], Pierre Lambert [b‡], Benoît Haut [b‡], Jonathan Goole [a‡*]

[a] Laboratoire de Pharmacie Galénique et de Biopharmacie, Université libre de Bruxelles (ULB), Brussels, Belgium
[b] TIPs (Transfers, Interfaces and Processes), Université libre de Bruxelles, Brussels, Belgium

Highlights

- A framework to develop nose-to-brain drugs combining pharmaceutics and engineering.
- The importance of the pre-formulation for safe, stable and efficient formulation.
- The selection of the administration device to target the olfactory zone.
- The 3D-printing of nasal casts to check the suitability of formulation properties.

Abstract

This review aims to cement three hot topics in drug delivery: (a) the pre-formulation of new products intended for nose-to-brain delivery ; (b) the development of nasal casts for studying the efficacy of potential new nose-to-brain delivery systems at the early of their development (pre-formulation); (c) the use of 3D printing based on a wide variety of materials (transparent, biocompatible, flexible) providing an unprecedented fabrication tool towards personalized medicine by printing nasal cast on-demand based on CT scans of patients.
This review intends to show the links between these three subjects. Indeed, the pathway selected to administrate the drug to the brain not only influence the formulation strategies to implement but also the design of the cast, to get the most convincing measures from it. Moreover, the design of the cast himself influences the choice of the 3D-printing technology, which, in its turn, bring more constraints to the nasal replica design. Consequently, the formulation of the drug, the cast preparation and its realisation should be thought of as a whole and not separately.

Keywords

Nose-to-brain, 3D printing, nasal casts, pre-formulation studies, administration devices, formulation properties, olfactory region, treatment effectiveness

†,‡ These authors contributed equally
* Corresponding author : jonathan.goole@ulb.be

doi: 10.1016/j.addr.2021.113826

Graphical abstract

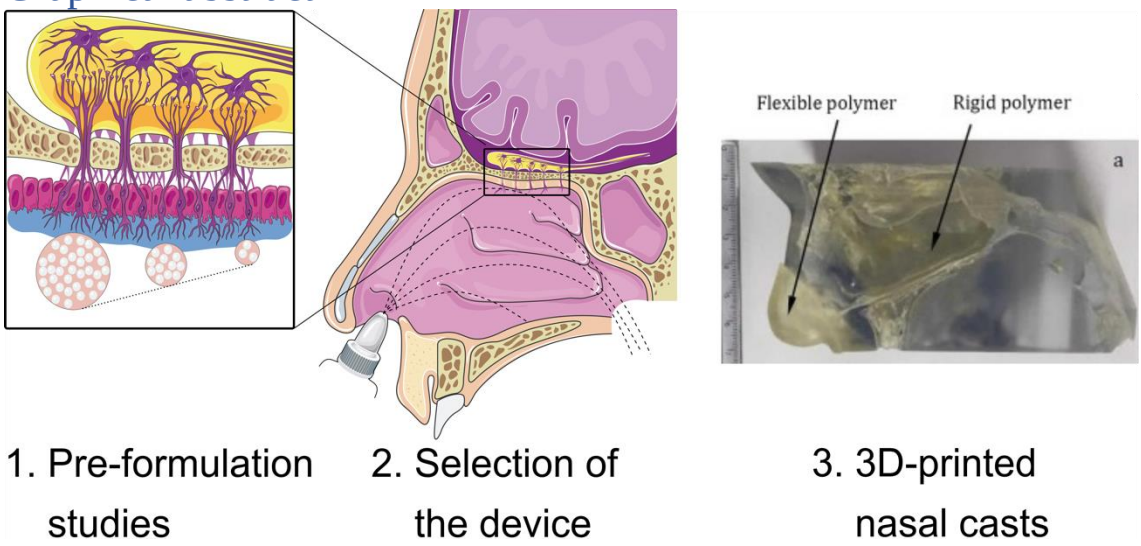

Table of contents

doi: 10.1016/j.addr.2021.113826

Introduction

Over the past few years, nose-to-brain (N2B) delivery has received growing interest. This method of administration is based on drug delivery in the nostrils to target the central nervous system (Figure 1). To reach the brain, the drug (Figure 1.1) must reach the olfactory zone (Figure 1.2 to 1.3), which are located at the top of the nasal cavities. Then, it must diffuse through the nasal mucosa (Figure 1.4) and the olfactory nerves towards the brain [1–3] (Figure 1.5). The main advantage of this N2B administration is its ability to bypass the systemic circulation. Therefore, it avoids potential enzymatic degradations due to hepatic first-pass and allows bypassing the blood-brain barrier. Moreover, it allows decreasing the therapeutic dose and the subsequent side effects [1–3]. This way of delivery is interesting in the treatment of severe brain pathologies such as tumours [4,5] or the treatment of degenerative neuronal disorder such as Parkinson's [6] and Alzheimer diseases [7,8].

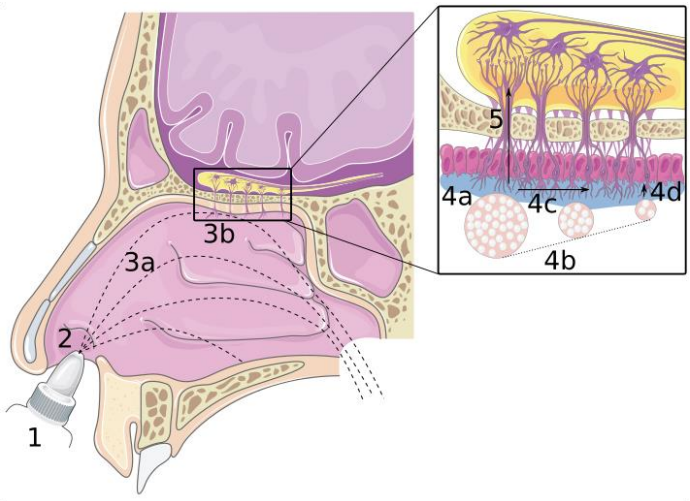

Figure 1: Principle of nose-to-brain delivery: (1) drug formulation; (2) instillation; (3) transport in the cavities and impaction of the mucosa: (4) transport in the olfactory mucosa: adhesion, dissolution, mucociliary clearance and diffusion; (5) transport through the epithelium and along the olfactory nerve. Source images by Servier Medical Art.

doi: 10.1016/j.addr.2021.113826

However, the N2B delivery of a drug is known to be challenging [9]. Indeed, the instillation of the drug into the nasal cavities must lead to the deposition of a significant fraction of the instilled dose in the olfactory zone [10,11]. It is far from being obvious, due to the complex geometry of these cavities, the olfactory region being in their upper part. Another option is to use the trigeminal nerve to get direct access to the brain [12]. The main advantage of using this second route is that the trigeminal nerve spans over the whole nasal cavity [13] and so the targeting is easier.

In both cases, while the drug diffuses through the nasal mucosa, the formulation must prevent any potential early degradation by enzymes [1,14–17] and its clearance by the natural beating of the cilia lining the epithelium of the nasal cavity [1–3,14,15].

Rigorous pre-formulation studies should be performed to face these challenges and succeed in the further development of an effective N2B formulation. In pre-formulation studies, the physicochemical properties of a drug candidate and its compatibility with excipients are characterized [2,7,14,15,18]. The goal of these studies is to increase the solubility and bioavailability of the drug. Pre-formulation studies also ensure good patient compliance to the treatment by selecting the right osmolarity (200-600 mOsm/l) [1] and pH (5-6.5) [1–3,19], improving the stability of the final product and guaranteeing an absence of toxicity. In N2B delivery, pre-formulation studies also aim at generating particles with a mean diameter such that a maximal fraction of the instilled dose can reach the brain. Such aerodynamic mean diameter is known to be dependent on the type of instillation device and the flow generated in the nasal cavities.

In addition to the pre-formulation studies, 3D-printed replicas of nasal cavities (so-called "nasal casts") are valuable tools. They allow making a link between the properties of a formulation candidate, the parameters of an administration device and the transport in the nasal cavities. Therefore, they can be used to ensure relevant targeting of the olfactory zone, which is a central element for the success of N2B therapy [20–26]. Such replicas should be 3D-printed with a material that is not porous and does not interfere with the quantification of a drug candidate during pre-formulation studies, as well as in quality control analysis. Moreover, the 3D printer should have a smooth surface and a sufficient resolution.

Next to "standard" nasal casts, casts may also be coated with artificial mucus to mimic the potential *in-vivo* behaviour of the impacting particles in an *in-vitro* device.

doi: 10.1016/j.addr.2021.113826

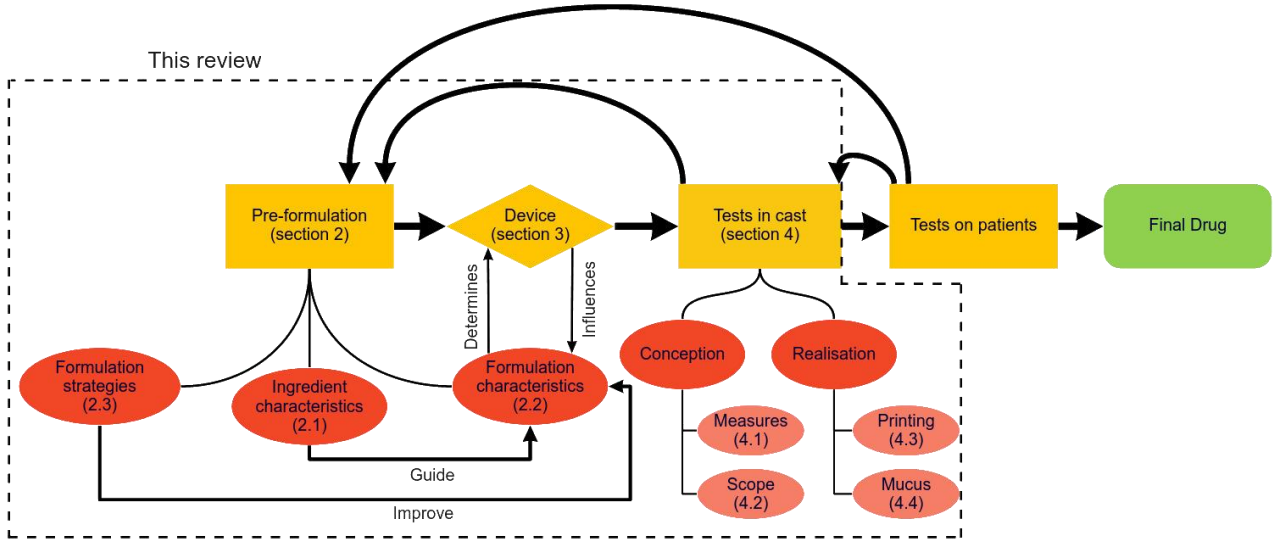

Figure 2: Steps in the development of a pharmaceutical product intended for nose-to-brain administration.

This review aims to provide a clear and global overview of the current knowledge and open questions regarding N2B delivery (Figure 2). There are three main stages: pre-formulation studies, device selection and tests in 3D-printed nasal casts.

The pre-formulation studies section focuses on the physio-chemical properties of the drug. It also illustrates the importance of pre-formulation studies to improve the proprieties of API and shows the final strategies to enhance the bioavailability of the formulation.

The section dedicated to the description of the devices describes the different instillators that are currently used and their influence on the success of the N2B treatments.

The 3D-printed nasal cast section describes the importance of designing the nasal casts following the constraints linked to the scope of the study. Then, it compares the different 3D printing techniques used for nasal replica production. Finally, it underlines the role of mucus in particle capture by the walls.

Due to the scarcity of available data [27], this paper does not focus on *in-vivo* studies and neither on the correlation between *in-vitro* and *in-vivo* data.

• Pre-formulation studies

This section describes the different steps to reach a safe, stable and efficient formulation (Figure 1.1). Indeed, treatments should be durable in time, safe for the patient and yield the appropriate therapeutic dose. The first step consists of identifying the physio-chemical proprieties drug candidates (e.g. solubility, partition coefficient, pKa, molecular weight) as

doi: 10.1016/j.addr.2021.113826

they can influence their solubilisation in mucus or their permeation through the olfactory epithelium [28–30].

To evaluate pre-formulation characteristics, there are three key targets: formulation stability, nasal mucosa preservation and treatment effectiveness. This part illustrates the importance of pre-formulation studies to improve N2B-drug properties [3,8].

Finally, this section exposes the approaches used to improve the bioavailability of formulation for N2B delivery. The strategy focuses on increasing drug bioavailability and decreasing mucociliary clearance and enzymatic degradation [1,2,17].

A summary of the pre-formulation studies workflow is described in Figure 3.

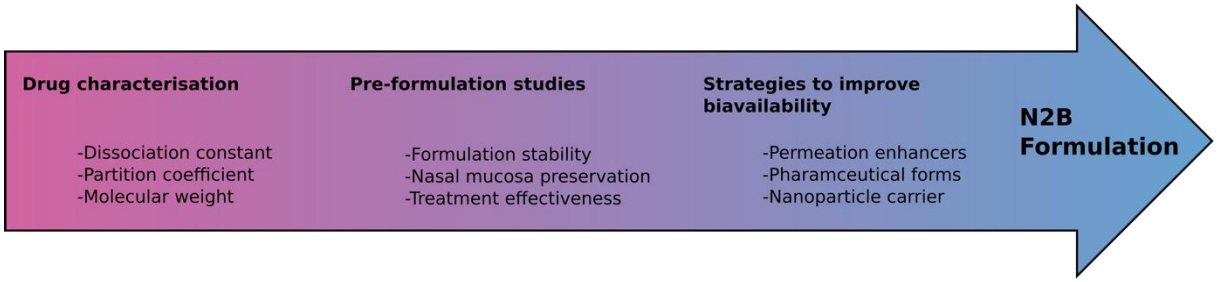

Figure 3: The active ingredient is first characterised in terms of acidic dissociation constant (pKa), partition coefficient (log P) and molecular weight (M_w). Then, pre-formulations studies aim to create a stable, safe and efficient formulation. Additional strategies (permeation enhancers, various pharmamceutical forms, nanocarriers) can be used to improve drug bioavalability.

○ Relevant physio-chemical proprieties of a drug regarding its N2B delivery

Several physio-chemical proprieties of a drug intended for N2B delivery should be identified at the early stage of the development, namely in the pre-formulation step. Indeed, they usually determine the strategy of formulation to adopt to further succeed in the development.

- *Solubility and absorption*

Solubility is the maximum quantity of a substance that can completely dissolve in a unit volume of solvent. The drug solubility is one of the essential factors to consider in pre-formulation studies since the drug must be dissolved to a large extent to diffuse through the mucosa and, then, through the olfactory region (i.e. through the olfactory nerves located in the cribriform plate [1–3]).

Moreover, N2B delivery involves the rapid dissolution of the instilled drug in a small liquid volume (between 50 and 150 µL). Indeed, drugs must be dissolved to be absorbed [19]. The

doi: 10.1016/j.addr.2021.113826

typical dose for a N2B drug is in the order of 20 µg [31]. So, their solubility should be at least 0.2 g/l to completely dissolve in the mucus layer and then be absorbed.
Several pre-formulation evaluations may be performed to evaluate the solubility of drugs in solvents, aqueous buffers or oils. The shake flask method [32,33] and the test tube method [34,35] enable determining this solubility. The solubility of an ionic drug correlates with its partition coefficient and its pKa.
After intranasal administration, the drugs must be absorbed through the olfactory epithelium to reach the brain [1–3,8,36–38]. The factors influencing the dissolution of the active ingredient (Hydrophilicity, pKa, Molecular weight) also control its absorption. So, the initial phase of pre-formulation studies should study these two aspects at once.

- *Intrinsic properties*

Partition coefficient

The partition coefficient of a drug describes its hydrophilic/lipophilic behaviour that influences both its solubility and its diffusion through the epithelium. Indeed, the higher the lipophilicity of the drug is, the easier it travels across epithelial cells [1,3,39]. The octanol/water partition coefficient (log P) describes drug hydrophobicity. The partition coefficient is the logarithm of the ratio of concentrations at equilibrium:

$$Log\ P = \log \frac{C_{octanol}}{C_{water}} \quad (1)$$

Thus, a lipophilic drug has a log P > 0, and a hydrophilic drug has a log P < 0. The larger this log P is, the more the drugs are lipophilic [40]. The hydrophilic drugs route is called the paracellular route. There is an inverse relationship between the molecular weight of the hydrophilic drug and its ability to diffuse between cells [1–3]. In N2B delivery, the transcellular route is the principal route for drugs absorption. Thus, lipophilic drugs are better absorbed than hydrophilic molecules [41]. The hydrophilic drugs have low permeability across the olfactory epithelium. Thus, it is necessary to use a pre-formulation strategy to bypass this limitation [41–43].
Indeed, *Giuliani et al.* compared the olfactory-bulb-to-plasma ratio of drug concentration for intravenous administration and the optimized formulation in nasal administration. The optimized formulation showed an olfactory-bulb-to-plasma ratio six times higher than the solution [42].

doi: 10.1016/j.addr.2021.113826

Salem et al. used lipidic nanoparticles to improve N2B delivery of their hydrophilic drug. The C_{max} in brain after intranasal administration of their nanoparticle formulation compared with the drug solution is 7 times higher (3.44 ± 0.03 µg/mL and 0.48 ± 0.04 µg/mL respectively) [44]

This demonstrates the importance of a suitable pre-formulation strategy to improve the bioavailability of hydrophilic API and the higher bioavailability of hydrophobic substances in N2B delivery.

pKa

The pKa is the pH at which the acid dissociates. This dissociation correlates with the solubilisation of the ionizable drugs and thus their absorption [28]. The proportion of ionized drugs depends on the nasal pH, usually ranged between 5.0 and 6.5 [1–3,19] and on its pKa. The Henderson-Hasselbach equation illustrates this relation:

$$pH = pKa + \log\frac{[B^-]}{[A^+]} \quad (2)$$

Equation 2 shows that if the drug pKa is lower than the pH of the formulation, the base form dominates. In contrast, if the pKa of the drug is higher than the pH of the formulation, the acid form dominates. For base drugs, the base form has no charge and the conjugate acid is cationic, while for acidic drugs, the acid form is neutral and the conjugated base is negatively charged [28,45].

For instance, levodopa is an anti-Parkinson acidic drug with pKa equal to 2.32. So, in the conditions described above, it will be mostly ionized. Risperidone is a basic drug with pKa equal to 8.76. Therefore, in nasal conditions, it will also be mostly ionized.

The lipophilic drugs have a poor dissolution rate in a small volume of nasal liquid. Thus, on their charged form, their solubility and their absorption increase [13,19]. Moreover, the cationic substances interact with negatively charged mucins of the nasal mucosa, which increase their affinity and remanence [37]. On the other hand, the hydrophilic drugs have a suitable dissolution rate [19]. However, the absorption in olfactory epithelium is better on their neutral form, [1,3,36]. Figure 4 shows a summary of dissolution and absorption of drugs as a function of their hydrophilicity and lipophilicity. As most acidic drugs have a low pKa and basic drugs have a high pKa, the most suitable drugs are lipophilic basic drugs (unionised if their pKa is lower than 5) and hydrophilic basic drugs (ionised if their pKa is higher than 6.5)

doi: 10.1016/j.addr.2021.113826

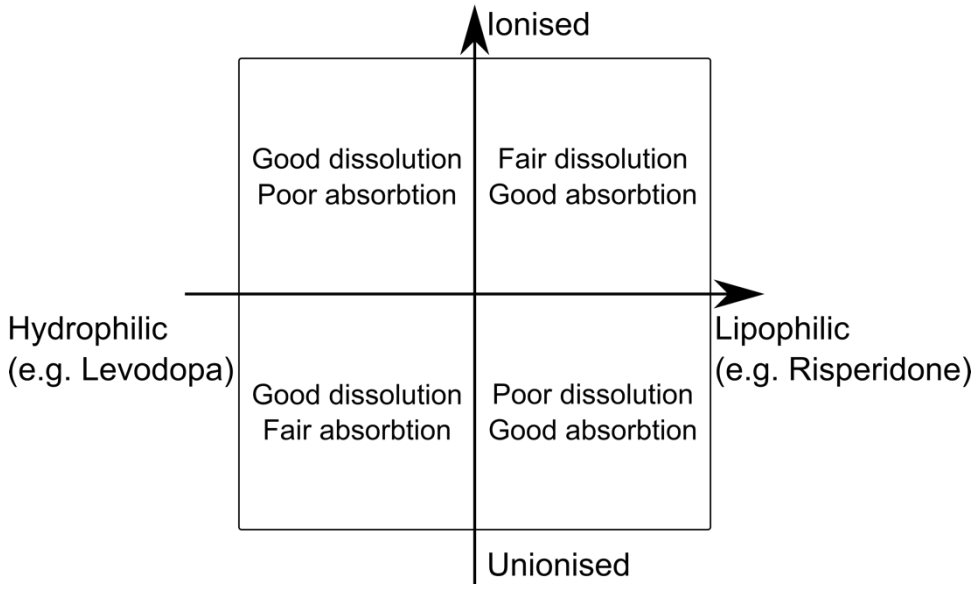

Figure 4: Suitability of a drug obtained by combining its dissolution and absorption properties.

Molecular weight

The drug absorption directly correlates with the molecular weight (M_w). Indeed, a drug with M_W higher than 1000 Da is usually characterized by poor absorption [1–3,37,38]. For lipophilic drugs, API with a M_w lower than 300 Da usually diffuse through passive diffusion. On the other hand, carrier-mediated transport is known to be used by molecules with a M_w ranged between 300 and 1000 Da [1,41].

For hydrophilic drugs, the absorption is directly proportionate to the M_w. Thus, their absorption rate proportionally decreases when the M_w is higher than 300 Da [1–3,41].

The correlation between molecular weight, lipophilic/hydrophilic behaviour of drug and percentage of drug absorption is illustrated in Figure 5.

A strategy to improve the bioavailability of macromolecular drugs (more than 1000 Da) in N2B delivery is the use of cell-penetrating peptide (CPP). *Lin et al.* explained the improved brain penetration of their CPP-protein nasal formulation by the macropinocytosis. Indeed, this CPP capacity allowed the drug to migrate deeply by saturating the cell layers one by one and so explained the drug diffusion by transcellular pathway [46]. *Yan et al.* compared the brain efficiency of their nanoparticles and their nanoparticles conjugated with CPP. They demonstrated a percentage 6 times higher for the CPP in olfactory bulb (0.405 % vs 2.64 %) and 3 times higher for the CPP in cerebrum (0.95 % vs 3.36 %) [47].

doi: 10.1016/j.addr.2021.113826

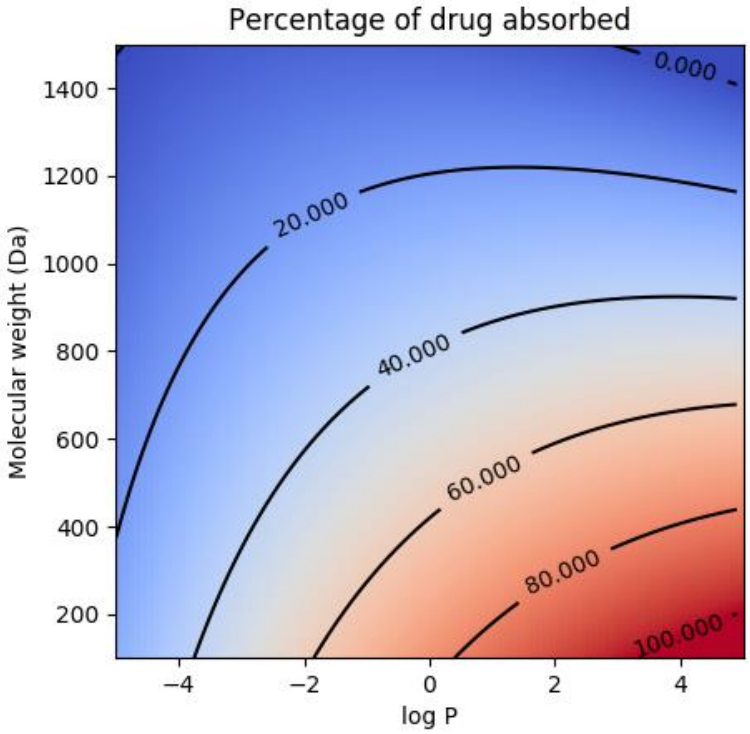

Figure 5: Iso-contour lines represent the percentage of drug absorbed as a function of its molecular weight and hydrophilicity/lipophilicity (log P)[48].

- The use of pre-formulation studies to improve properties of drug attended in N2B delivery

Pre-formulation describes both physicochemical properties and kinetic rate profile of a new drug (i.e. its outcome in the organism) [49]. It also evaluates the compatibility between drugs and excipients as well as the processability of the drug.

The physicochemical properties of the drug indicate paths to improve the pH, osmolarity and viscosity of the formulation. Osmolarity is the mass of solute which, when dissolved in 1 litre of solution, will exert an osmotic pressure equal to the pressure exerted by a mole of an ideal unionized substance dissolved in 1 litre of solution [50]. Viscosity is the resistance of a fluid to motion [51].

Then, according to the inherent properties of the candidates, researchers can develop a formulation strategy (Figure 6). This strategy increases the impaction of the formulation onto the olfactive region as well as the diffusion of the drug through the neuroepithelium. To this end, it is crucial to assess the compatibility between the drug and the excipients. Similarly, researchers should also evaluate the potential toxicity of the final formulation. Moreover, pre-formulation also aims to improve the stability of a developed formulation through production and long-term storage.

doi: 10.1016/j.addr.2021.113826

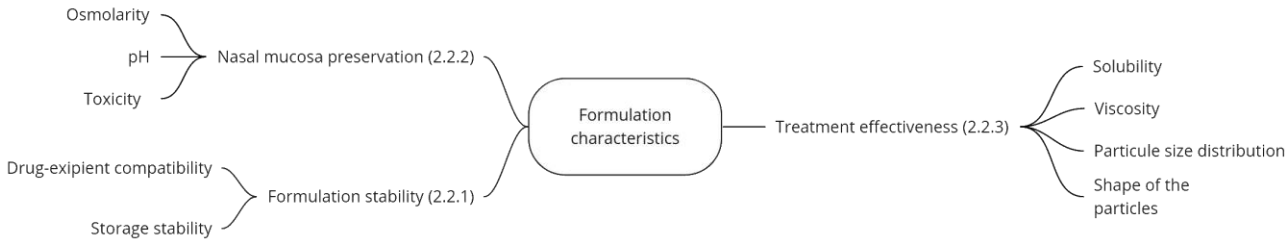

Figure 6: Formulation characteristics impacting final N2B treatment.

- *Formulation stability*

Drug-excipients compatibility

It is crucial to evaluate the compatibility between drugs and excipients. For instance, Fourier Transform Infrared (FTIR) spectroscopy allows assessing any potential interaction between both [52–56]. X-Ray Diffraction (XRD) study is used to evaluate the proportion of crystallinity or amorphous state and the encapsulation of drug in the formulation or polymorphic changes [53,55,57,58]. Another way to evaluate compatibility is thermal analysis. Differential Scanning Calorimetry (DSC) enables the investigation of drug-excipients interaction, polymorphic transition. It also permits checking the encapsulation of the drug by thermal modification [53,55,58–62].

Stability during storage

The nasal formulation must ensure the stability of the drug over time during storage. It also covers the physical and chemical stability of the prepared emulsion, suspensions or solutions (in the case of liquid formulation).

This stability may be obtained using several strategies. For liquid formulations, it can be advised to add antioxidant (e.g oxidizable API/excipients) and antimicrobial agents. But this kind of substances may be irritant or allergenic for the patient [63–66]. *Rodriguez et al.* demonstrated the importance of the choice of antioxidants in liquid formulations. Indeed, they studied the antioxidant activity of different antioxidants for levodopa. The autoxidation of this molecule causes the liberation of free radicals. These free radicals are responsible for oxidative stress-induced cytotoxicity. Their pre-formulation studies allowed them to select the best antioxidant in low concentration [67]. It is possible to avoid the use of such preservatives with the development of dry formulations. Those formulations were already described to increase the stability of vaccines [64–66].

doi: 10.1016/j.addr.2021.113826

Another point to evaluate is the potential degradation of the instilled drug by the enzymes present in the intranasal cavity. For instance, these enzymes are carboxylesterase, aldehyde dehydrogenases or cytochrome P450. Such enzymatic degradation could lead to a decrease in drug diffusion through the neuroepithelium and the efficacy of the treatment. It can be overcome by using enzymatic inhibitors such as comostate [16,17].

The final point to discuss is the colloidal stability of dispersed systems. Colloidal stability may be evaluated by measuring the zeta potential of the formulation. A zeta potential above +20 mV or below -20mV indicates that the colloidal system is stable [37]. Other means to describe colloidal systems stability are the particles size distribution and the polydispersity index (PDI). Indeed, the polydispersity index is a measure of the heterogeneity of a sample based on its size distribution. Indeed, a colloidal system has a narrow particle size distribution with PDI values ranged between 0.1-0.2 [68]. Stability can be increased with the use of a steric stabilizer [69]. *Shudin et al.* illustrated the importance of pre-formulation to improve colloidal stability. They studied the influence of pH, the different ratio of constituent and the fabrication process. They considered the nanoparticles size and the polydispersity index to be minimal and the zeta potential to be maximal [70]. This kind of pre-formulation studies is helpful during nanoparticle's developments [53–56,62,71–74]. It allows researchers to select the most stable formulation and the optimum particles size for N2B delivery. Indeed, effective brain targeting has been reported for particles size lower than 200 nm [53,72].

- *Nasal mucosa preservation*

Osmolarity

The osmolarity of the formulation is also of great importance in N2B delivery. Several teams studied the influence of osmolarity in the bioavailability of drugs and they concluded to a better bioavailability for hypotonic formulation. *Pujara et al.* studied the release profile of lactate dehydrogenase (LDH) from the rat nasal cavity as a function of formulation osmolarity [75]. Only the hypotonic solution demonstrated a high amount of LDH release. Indeed, hypotonic solutions cause the swelling of the epithelial cells and increase water uptake. On the other hand, the hypertonic solutions cause shrinkage of the cells and reduce the chance of release. *Dua et al.* studied the administration of isotonic, hypertonic and hypotonic salmon calcitonin solution in rabbits [76]. They showed that for low-viscosity solutions, the isotonic formulation was far less efficient than the two others and for high-viscosity solutions, it was the hypertonic one that was the less efficient. So, on average, they also conclude that the

doi: 10.1016/j.addr.2021.113826

hypertonic formulation should be preferred. Finally, *Olivier et al.* showed no influence of solution osmolarity when giving midazolam to rats, except if it was less than 10 mOsm/l [77].

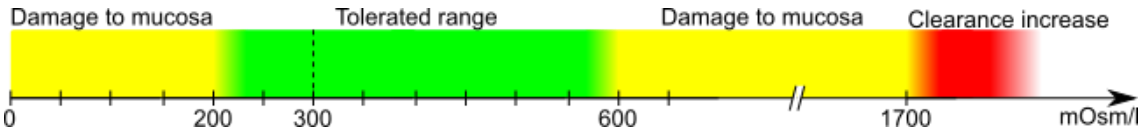

Figure 7: Tolerated osmolarity for nasal formulations.

However, the formulation should range between 200 and 600 mOsm/l to preserve the integrity of the nasal mucosa (**Erreur ! Source du renvoi introuvable.**) [1]. These alterations would lead to a potential toxic effect in chronic therapy [3]. Finally, hypertonic formulations activate the mucociliary clearance, which increases the elimination of the drug. However, this effect is significant only at 1700 mOsm/l [78]. In conclusion, hypotonicity is often sought in formulations to increase the drug absorption but researchers should ensure not induce in this way any toxicity for the mucosa.

pH

As explained previously, the pH of the formulation influence drugs ionization and stability [37]. *Olivier et al.* perfectly illustrated this point. Indeed, they studied the pH of nasal formulation influence in midazolam absorption. They demonstrated an efficient absorption in pH 5.5 and 7.4 compared with pH 3.3. Indeed, the percentage of unionized form is 20 % and 95 % in pH 5.5 and 7.4 respectively. In the lowest pH values, the proportion of unionized form is poor and thus the absorption decrease [77].

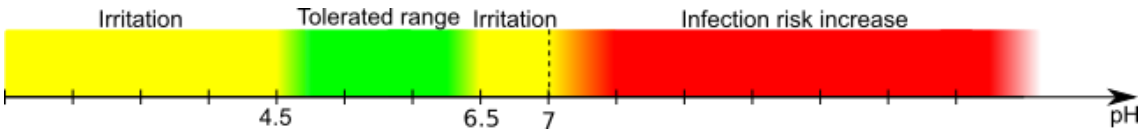

Figure 8: Tolerated pH range for nasal formulations.

But apart from the influence on the API, the pharmaceutical forms must respect a range of pH. In fact, for intranasal administration, the pH of the liquid form or the powder form after dissolution must be between 4.5 and 6.5 to be well tolerated (Figure 8) [1–3,19]. An increase in pH promotes the risk of infections in the nasal cavity as it may inhibit the lysozymes in charge of destroying them [1,37,41].

Toxicity

The FDA's website provides an Inactive Ingredients Database that contains a list of excipients that may be used according to the administration route and the tolerated dose [79].
Moreover, histological evaluations allow the evaluation of ciliotoxicity or mucosal toxicity [55,80–83]. *Wang et al*. studied the nasal ciliotoxicity of rotigotine-loaded polymeric micelles in thermosensitive hydrogels. They evaluated the duration of cilia movement after formulation exposition and the inflammatory state of the tissue. No significant modification of the cilia movement duration was observed between the control solution and the drug-loaded formulation: respectively 599 ± 16 min and 554 ± 25min. And for the nasal tissue integrity, they measured that the duration of the cilia movement after formulation application was 92.5% of the duration before application. They considered that the drug and its excipients had no apparent damage to the cilia movement [80]. Therefore, these pre-formulation studies confirmed the safety of their formulation before the *in-vivo* studies.
Another preclinical analysis evaluated the toxicity of the pre-formulation is to evaluate cell viability [55,73,82,84]. *Kim et al.* used the MTT assay to assess the toxicity of their formulation. Indeed, the use of permeation enhancers may lead to higher bioavailability of drugs. However, their potential toxicity to the mucosal site after repeated administration restricts their further applications. Thus, they proved a low reduction of relative cell viability after 24h contact between their formulation and the RPMI2650 cell line (more than 70% of cell viability) [82]. This kind of pre-formulation study should be used to choose the safest excipient for N2B formulation. *Kim et al.* also used a more specifically pre-formulation analysis for N2B delivery. They made primary neuronal cell culture with rats. *In vitro* optical microscopy was performed to observe the effect of their formulation on the morphology of primary neurons to validate the safety of the formulation [82].

- *Treatment effectiveness*

Solubility
A lack of solubility usually decreases the absorption of a drug as it has to dissolve in the nasal mucosa, which retains a low volume of aqueous fluids (between 50-150 µL) [19]. Several strategies may be used to improve the solubility of a poorly soluble drug, such as the use of surfactants, cosolvents or buffers [1–3,15].
In contrast, although their high solubility, hydrophilic drugs face one major issue in N2B delivery. Their high solubility in the mucus and their slow permeation across the membrane [2] involve their relatively fast elimination by mucociliary clearance. Indeed, the mucus layer renews approximately every 15-20 minutes [15,37].

doi: 10.1016/j.addr.2021.113826

Viscosity

The viscosity of the formulation greatly contributes to increasing drug absorption. Viscosity has two effects on absorption. A properly selected viscosity decreases the mucociliary clearance (MCC) and increases the residence time as well as the absorption of drugs [1–3,37]. In contrast, excessive viscosity may decrease drug diffusion through the formulation and the olfactory region [37,85]. Stokes-Einstein equation illustrates this phenomenon:

$$D = \frac{kT}{6\pi\eta a} \quad (3)$$

where D = diffusion coefficient; k = Boltzmann constant; T = absolute temperature; η = viscosity of the medium/solvent; a = molecular radius.

According to equation 3, the more the viscosity increases, the more the diffusion coefficient decreases [85]. This point illustrates the importance of a pre-formulation study because researchers must develop a sufficiently viscous formulation to decrease the MCC but not too much to obtain an efficient release of API.

Furubayashi et al. studied the effect of viscosity formulations (between 1.2 and 147.11 mPa.s) in nasal absorption and MCC in rats. They confirmed that an increase in the viscosity increases the mean resistance time of the formulation in rat nasal cavities. But for the most viscous formulation (147.11 mPa.s), the nasal absorption decreases approximatively by 30% in comparison to the control formulation [86]. *Pires et al*. studied the influence of formulation viscosity in drug release in their pre-formulations studies to select their optimum formulation for *in vivo* pharmacokinetic analysis. They demonstrated that, for similar formulations, the most viscous (~ 154 Pa.s) had the lowest percentage of drug release (approximatively 10% less than the control at the end of the experiment) [87].

For liquid formulations, the second important part is the influence of viscosity in the device. Indeed, viscosity modifies the plume angle and the targeting properties of the formulation [24,25,88–90]. *Pu et al.* added microcrystalline cellulose (Avicel®) or hydroxypropyl methylcellulose (HPMC) to aqueous mometasone furoate solutions to sweep viscosities from 1.3 to 21.8 cP. Adding 2% w/w of Avicel® in solution increased the viscosity by a factor of 17 while the plume angle diminished from 50° to 46°. Similarly, adding 0.3% w/w of HPMC made the plume angle drop by 12° while multiplying the viscosity by 6 [89]. Also, *Warnken et al.* added HPMC in cromolyn sodium nasal solution to increase the viscosity from 1 to 53.1 cP. At the same time, the plume angle dropped from 48° to 24° [24].

doi: 10.1016/j.addr.2021.113826

Particle size distribution

The particle size distribution is another important parameter to evaluate when the administration aims to target the olfactory region. For dry powders, several studies concluded that a mean diameter around 10 µm maximises the amount of powder that could impact the olfactory zone [11,91]. In a recent paper, *Yarragudi et al.* studied the deposition efficiency in the olfactory region. They compared two different models of devices: nebulizer, propelling the particles in a single nostril, and bi-directional airflow, creating a circulating airflow across the two sides of the nose. They concluded that the ideal mean diameter should be ranged from 8 to 12 µm [10]. Similarly, *Schroeter et al.* found that 10 µm particles are the most efficient mean diameter to reach the olfactory zone. It underlines the importance of a pre-formulation step taking into account particle size to obtain particles adapted for nose-to-brain delivery.
For the N2B delivery, liquid formulations seem to be less efficient than the dried systems [24,92–94]. *Calmet et al.* studied, via computer simulations, the nasal deposition in the olfactory region of nasal sprayed particles under different simulated inspirations. They demonstrated the same conclusions as previous studies: the use of a liquid formulation for N2B delivery is inefficient [92]. Other teams also concluded an ineffective deposition on the upper turbinate region with a nasal liquid spray: *Warnken et al.* observed a maximum olfactory fraction of 2.2% of the emitted dose [24], and *Shah et al.* find only about 0.4% of the emitted drug in the olfactory region [93]. *Kiaee et al.* concluded the same inefficiency, but they demonstrated a maximal deposition efficiency in everyday-life usage conditions in the turbinates for particle size ranging between 20-30 µm [94]. It worth noting that liquid formulation however provides rather good results in animals [95–97]. However, these studies do not rely on a spray to administrate the formulation but directly irrigate the cavities. Consequently, particle size produced while delivered to a human does not play any role there.

Shape of the particles

As previously discussed, the evaluation of the particle size distribution is crucial to get an efficient N2B formulation. The diameter to consider is the aerodynamic diameter which is be defined as follow:

$$d_{ae} = d_{geo}\sqrt{\frac{\rho_p}{\rho_0 \chi}} \quad (4)$$

where d_{geo} is the geometrical diameter of the particle, ρ_p its density, ρ_0 the density of water (1000 kg/m³) and χ the dynamic shape factor, which is the ratio between the resistance force

doi: 10.1016/j.addr.2021.113826

exerted on the irregular particle and a spherical particle having the same volume and velocity [98]. It is the aerodynamic diameter and not the geometric diameter that influences the path followed by the particles in the nose.

In the ideal situation, the particles have a spherical shape. Indeed, this shape leads to lower flow resistance for the same geometric diameter [99]. Consequently, it is crucial to select the most efficient fabrication method (e.g. spray-drying). Despite a proper choice for the fabrication method, it is impossible to have only spherical particles. Indeed, the particles almost always have an irregular surface, including voids and holes [98].

For observing particle morphology, Scanning Electron Microscopy (SEM) is a usual method [52,100–102]. SEM is helpful in addition to a laser diffraction analysis because this last method does not allow knowing the morphology of particles but only their size distribution. Moreover, the SEM (resolution down to a few nm) [103] outperforms optical microscopy (resolution about 200 nm) [104].

Spherical morphology is also suitable to reduce interparticle cohesiveness. It also ensures a good flowability of blends [102]. Low cohesiveness and good flowability are two characteristics required for a repeatable device filling [105].

○ Use of strategies to improve bioavailability

Several formulation approaches exist to improve the cerebral bioavailability of drugs (i.e. the proportion of API in the brain). The choice of a strategy depends, of course, on the drug physicochemical properties. Pre-formulation studies validated the added value of the use of these strategies.

▪ *Barriers to drug absorption*

An efficient intracerebral bioavailability of N2B formulation depends on two main factors: their residence time in the olfactory region and the mucociliary clearance. When the residence time is increased, and the mucociliary clearance is decreased, the diffusion through the olfactory membrane increases (Figure 1.4). Thus, a higher concentration of the drug is achieved in the brain (Figure 1.5). These factors are interconnected, and a good knowledge of them is mandatory to develop N2B formulations. The most commonly used method for studying drug concentration in the brain is the drug dosage in brain tissue from sacrificed animals [56,61,62,74,80,82,84].

doi: 10.1016/j.addr.2021.113826

Residence time

The residence time may be increased by enhancing mucosal affinity. The mucosal affinity may be increased using mucoadhesive agents, which strongly interact with mucins that are located in the olfactory region [37]. The residence time greatly depends on mucociliary clearance. If mucociliary clearance is decreased, the residence time increases [1–3,14,15].

Mucociliary clearance

The mucociliary clearance is the main restricting factor of absorption of the active ingredient in the nasal cavity. It is the predominant defence mechanism in the nose. Exogeneous materials, such as microorganisms, pollutants or drugs, are trapped in the mucus layer. Then, they are transported to the nasopharynx due to ciliary movements [2]. The mucociliary clearance in humans is around 8mm/min. The normal mucociliary transit ranges between 12-15 min [14,15,19,37]. It is reported that a mucociliary transit greater than 30 minutes may be considered abnormal and could signify a potential alteration of the nasal mucosa [106]. Another crucial point about mucociliary clearance is its dependence on the region of nasal cavities. For instance, the posterior part has more cilia than the anterior part of nasal cavities, hence a faster clearance. In contrast, the olfactory region is characterized by long and non-motile cilia which do not participate in mucociliary clearance [107–109]. Therefore, the region of deposition of the drug has a significant effect on its absorption and bioavailability [2,37].

Epithelial permeation

The permeation through the nasal epithelium is essential to get a high absorption of the drug and thus increased bioavailability. In general, the intranasal route is efficient for substances with a molecular weight lower than 1000 Da and a particles size lower than 1 µm [2]. Different barriers limit the mechanisms of drugs absorption via N2B delivery. The first limiting factor is the mucus layer. The drugs must dissolve or pass through the mucus layer before being eliminated by the mucociliary clearance or attacked by enzymes [1,13,15]. The mucus layer renews in 15-20 minutes [15]. The small neutral molecules are quickly dissolved in the nasal mucus [1].

Then, the formulations must pass through the olfactory epithelium. This epithelium is constituted by pseudostratified columnar cells interconnected via thigh junctions. It is crossed by the axons of olfactory neurons [13,15]. There exist two main ways to pass this epithelium: paracellular route and transcellular route [1–3,13,15,110] (Figure 9).

doi: 10.1016/j.addr.2021.113826

The transcellular route is the lipoidal way. The absorption by this route increases with the lipophilia of the molecule and decreases with its molecular weight. Substances greater than 1000 Da has poor bioavailability [1–3,37]. This way includes several transport mechanisms: passive diffusion, carrier-mediated transporter or endocytose (for substances higher than 1000 Da) [1–3,13,15,110]. The passive diffusion in the transcellular route is adapted to lipophilic substances less than 1000 Da [1,2,13]. The carrier-mediated path mainly involves transporters. P-glycoprotein, organic cation transporter, dopamine transporter, and amino acid transporters are predominantly expressed in the olfactory [2]. When the drugs have a molecular weight larger than 1000Da, they are mainly absorbed by endocytosis [2]. This mechanism concerns proteins, peptides as well as nanostructures greater than 500nm.
The paracellular route is the route of small hydrophilic substances (less than 1000Da)[1–3,13,15,110]. It involves a passive diffusion across aqueous spaces between cells. So, this diffusion decreases with the molecular weight increase [1,2,14,15]. The main limitation of this way is the presence of thigh junctions. But to increase the permeation across there, permeation enhancers (chitosan, cyclodextrins) can be used to open thigh junctions [1–3,14,15,18].

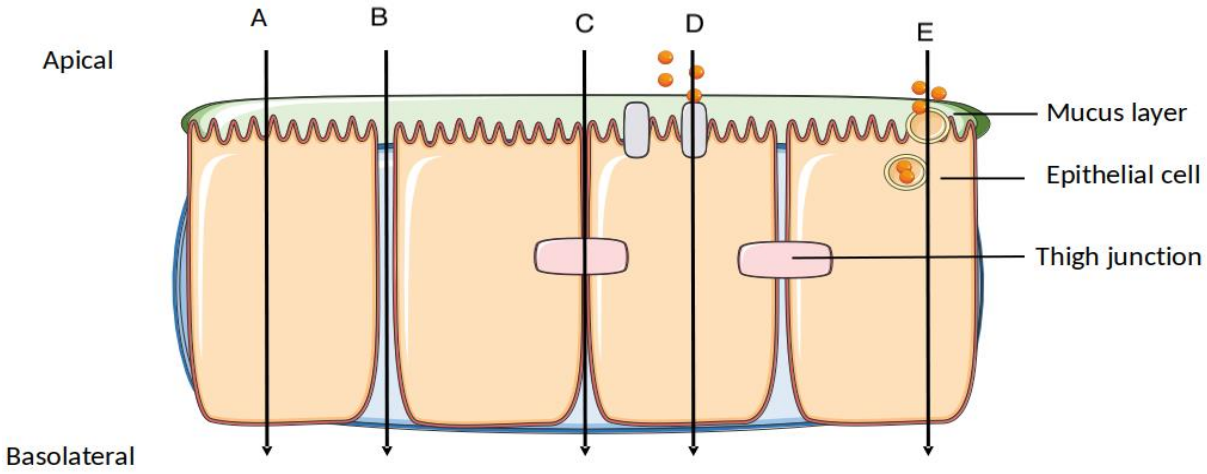

Figure 9: Mechanism of drugs transport through the nasal epithelium from the apical to basolateral side: (A) passive diffusion in transcellular route, (B) intercellular diffusion in paracellular route, (C) thigh junction diffusion in transcellular route, (D) active transport and (E) endocytosis. Source images by Servier Medical Art.

- *Permeation enhancers*

The use of permeation enhancers aims to increase the absorption of drugs through the olfactory epithelium. Such excipients improve the bioavailability of drugs due to their unique properties, which include mucoadhesion, enzymatic inhibition, thigh junctions opening or

solubility enhancement [1–3,7,15,18,111]. Moreover, some are characterized by more than one of these properties, such as bile salts, chitosan and cyclodextrins derivatives [3].
Chitosan derivatives are widely described to improve drug absorption in N2B delivery [72,112,113]. They are natural polymers, biocompatible, biodegradable and non-toxic. Nevertheless, as they all derivate from crustacea shells, particular attention must be paid to allergenic properties. The permeation enhancement properties of chitosan derivatives greatly depend on their molecular weight, deacetylation degree and purity [114]. Moreover, these derivatives improve the absorption of the drugs in the olfactory epithelium according to several strategies. It has mucoadhesive properties and can open the thigh junctions, which enhance paracellular absorption. Indeed, the chitosan generates dehydration of epithelial cells, which causes an opening of thigh junctions [110,115]. Besides, this dehydration is supported by an increase in formulation viscosity, leading to an increased residence time. And finally, the chitosan generates electrostatic interactions between positive charges of its amino groups and negative charges of glycans of mucus. That increase the affinity with olfactory epithelium and decrease the mucociliary clearance [116]. A recent complete study, conducted by *Bhattamisra et al.*, demonstrated the benefits of chitosan for N2B delivery. They carried out pharmacodynamic and pharmacokinetic (PK) pre-formulation studies in rats. Their PK study illustrated a significant increase in brain concentration with rotigotine-loaded chitosan formulation compared with an aqueous solution of rotigotine: 61.72 ± 7.44 ng/ml and 36.74 ± 23.41 ng/ml, respectively. Their pre-formulation demonstrated the favourable proprieties of this permeation enhancer to improve brain bioavailability [72].
Cyclodextrin derivatives may also be used as permeation enhancers in N2B delivery [55,84,117]. *Belgamwar et al.* demonstrated the efficiency of the use of cyclodextrin NPs for N2B delivery. Indeed, the intranasal administration of NPs in rats showed a higher C_{max} compared to drug solution in intravenous and intranasal administration (24.90 ± 4.56 µg/mL, 8.19 ± 1.12 µg/mL and 19.90 ± 4.08 µg/mL respectively [55]. Cyclodextrins are cyclic oligosaccharides with a toroidal form with units of glucopyranose. They have an internal lipophilic part and an extern hydrophilic part [84,118]. Cyclodextrins may remove the phospholipids and the cholesterol from the cellular membrane, which increase its permeability and the absorption of the drug. They also influence the distribution of specific proteins constituting the thigh junctions, increasing drugs absorption through the paracellular route [119]. A final advantage of their use is their ability to increase the apparent solubility of poorly soluble drugs [118].

doi: 10.1016/j.addr.2021.113826

Several other permeation enhancers increase the absorption of the API through N2B delivery [120]. For instance, bile salts can open the thigh junctions and inhibit the enzymes, fatty acids may disrupt the plasmatic membrane, cellulose derivatives usually decrease the mucociliary clearance by increasing the viscosity of the formulation [3] and surfactants improve the solubility and transport of hydrophilic molucules across the nasal epithelium [121].

- *Pharmaceutical forms*

For N2B delivery, three pharmaceutical states are usually used: liquid formulation, powder formulation and gel formulation. The main advantages and disadvantages of these different forms are illustrated in Table 1. As already mentioned, it has been demonstrated that dried powder formulations have more advantages than liquid formulations [63,65,122,123].
The pre-formulation studies could demonstrate the advantages of pharmaceuticals form in terms of bioavailability. Indeed, *Fransen et al.* demonstrated that dry powder formulations exhibited a greater bioavailability than nasal liquid formulations. The C_{max} of intranasal liquid and powder spray are respectively 34.1 and 103.3 pg/mL. Such observation was explained by the increase of the residence time in nasal mucosae for the dry formulations. Indeed, the mucoadhesive proprieties of powder decreased the mucociliary clearance. This fact has been confirmed by patients, who declared that the powder did not run down the throat. Also, the nasal dry powder formulations contained starch as permeation enhancers. The starch can increase paracellular absorption of the drugs by opening thigh junctions [123]. Moreover, *Vasa et al.* demonstrated the importance of powder granulometry on nasal dry powder mucoadhesion. Indeed, the micronation of nasal dry powder allowed to rapidly reaching the saturated concentration of drugs on the nasal epithelium surface. That explained the higher permeation through the membrane for dry formulations compared to liquid formulations. For this pre-formulation study, they selected microparticles with a particles size of lower than 20 µm [63]. Indeed, olfactory deposition is optimum in the range of 8-12 µm [10,124].
Another relevant advantage of powder drug-loaded formulation is its higher stability, which makes them a relevant candidate in vaccines development [125].
A recent kind of pharmaceutical forms described in the literature for N2B delivery is stimuli-responsive gels. Such systems can transit from solution to gel in response to a stimulus (e.g. pH, temperature or magnetic field) [126,127]. The main advantage of them in comparison with liquid forms is their capacity to increase the residence time on the nasal epithelium and increase the drug bioavailability. This advantage comes from their higher viscosity and their ability to swell upon contact with biological fluids. Moreover, their administration seems

doi: 10.1016/j.addr.2021.113826

easier as they allowed using a liquid form, in easy-to-use devices, which swell thanks to a targeted stimulus [128].

Let us also mention that the vast majority of nasal products commercially available are liquid formulation. Up to now, only a few powders (e.g. Baqsimi®, Inbrija®, Onzetra®) or gels (e.g. Vibrosil®, Natesto®) have been approved for nasal administration.

Table 1: Advantages/Disadvantages of pharmaceutical forms in N2B delivery: (+++) excellent, (++) fair, (-) poor.

States	**Stability**	**Preservatives**	**Bioavailability**	**Easy to use**	**Targeting the olfactory region**
Solid [2,3,122]	+++	none	+++ Decrease MCC Increase resident time	++ Discomfort during administration	+++ Controlled particle size
Liquid [2,3]	-	- Allergenic Irritant	- Rapidly eliminate by MCC	+++	- High deposition in anterior cavities
Gelling [2,3,126]	-	- Allergenic Irritant	+++ Decrease MCC Increase resident time	+++	++ Use of stimuli responsive gels

- *Nanoparticles*

The use of nanocarriers is a novel strategy to improve drugs bioavailability in N2B delivery. For this purpose, three families of nanoparticles (NPs) are commonly described: polymers-based NPs, lipid-based NPs and hybrid systems (Table 2) [1,14,15,129]. The main advantage of this kind of particles is their range of particles size. The nanocarriers are a colloidal system with a mean hydrodynamic diameter ranging between 1 and 1000 nm [37,129]. Such particle size distribution promotes transcellular transport to the brain. They are also used to encapsulate the drugs and protect them from enzymatic degradations [1–3,14,15,129]. The other advantages are more specific and depend on the type of NPs.

Poly(lactide-co-glycolide) acid derivatives (PLGA) are extensively used to formulate polymers-based NPs for N2B delivery and are also approved by the FDA as a potential drug

doi: 10.1016/j.addr.2021.113826

carrier. Their main advantage is their ability to properly control the drug release by modification of their molecular weight and the ratio between polylactic and glycolic acid functions. And their modification is easy to accommodate their target region [72]. *Arisoy et al.* demonstrated that the use of Levodopa-loaded PLGA nanoparticles could be a new efficient treatment for Parkinson Disease. Indeed, they compared the dopamine levels in the brain after intranasal administration of levodopa and levodopa-loaded NPs in male mice. They observed an increase of around 16% of brain dopamine levels for the levodopa-loaded NPs [62].

Lipid-based NPs are considered the most efficient NPs for N2B delivery. Indeed, they protect the drugs from extracellular transport by efflux proteins, biological, enzymatic and chemical degradation. Their lipidic functions also exalt their biocompatibility and biodegradability properties. [130]. The nanostructured lipid carriers (NLCs) are the new generation of lipid-based NPs. The lipid compound allowed increasing the drugs loading in comparison with the first generation of lipid NPs. These lipid compounds are composed of a solid lipid part and an oil part [129]. *Masjedi et al.* studied the pharmacokinetics of sumatriptan-loaded NLC for migraine treatment. They proved the significantly higher concentration of sumatriptan in the brain for NCL formulations. Absolute brain bioavailability between sumatriptan free and nanocarriers increase by a factor of 4.4. Therefore, such formulation strategies seem to be promising to treat migraine in the future [61].

Table 2: Recent type of NPs used in N2B delivery and their characteristics (particle size (PS), PDI, zetapotential (ZP), entrapment efficiency (EE) and drug content DC).

Nanoparticles	**Type of nanocarrier**	**Drug-Pathology**	**References**	**PS (nm)**	**PDI**	**ZP (mV)**	**EE %**	**DC %**
Polymer-based NPs	TPGS micelle	Curcumin-Anticancer	*Keshari et al.* [71]	*146.8*	*0.189*	*-22.5*	*98.19*	*1.935*
	PAMAM dendrimer	Donepezil-Alzheimer's disease	*Singh et al.* [56]	*122 ± 1.88*	*0.434 ± 0.322*	-	-	-
	Chitosan	Rotigotine-Parkinson's disease	*Bhattamisra et al.* [72]	*72.37 ± 3.37*	*0.368 ± 0.02*	*+25.53 ± 0.45*	*96.08 ± 0.01*	-

	PLGA	Levodopa-Parkinson's disease	*Arisoy et al.* [62]	*383.7 ± 66.94*	*0.426 ± 0.195*	*- 20.8 ± 3.63*	*50.47*	-
	Hydroxypropyl-betacyclodextrin	Dolutegravir-HIV	*Belgamwar et al.* [55]	*81.94 ± 3.7*	-	*- 18.7 ± 2.1*	*77 ± 3.36*	*14.9 ± 0.7*
Lipid-based NPs	Solid lipid NPs	Rotigotine-Parkinson's disease	*Prajapati et al.* [53]	*129*	*0.285*	*- 23.1*	*83*	*87*
		Dopamine-Parkinson's disease	*Cometa et al.* [54]	*147 ± 24*	*0.44-0.58*	*+ 5.2 ± 1.7*	*81 ± 2*	-
		Zulmitriptan-Migraine	*Mostafa et al.* [83]	*249 ± 22.77*	*0.41 ± 0.56*	*- 12 ± 1.54*	*76 ± 1.34*	-
	Nanostructured lipid carriers (NLCs)	Sumatriptan-Migraine	*Masjedi et al.* [61]	*100*	*0.27*	*- 32 ± 0.4*	*91.00*	*5.90*
		Cannabidiol-Neuropathic pain	*Matarazzo et al.* [58]	*177 ± 3.1*	*0.30 ± 0.02*	*+ 41 ± 0.6*	*99.99 ± 0.0001*	*18.75 ± 0.0001*
		Rivastigmine-Alzheimer's disease	*Cunha et al.* [131]	*109.000 ± 0.850*	*0.196 ± 0.007*	*- 30.466 ± 0.252*	*97.174 ± 0.297*	-
	Liposomes	Baicalin-Cerebral Ischemia	*Xiang et al.* [132]	-	-	-	-	-
		Rizatriptan-Migraine	*Padalkar et al.* [133]	194 ± 22.7	*0.5*	*+ 5.90 ± 0.1*	*84.9 ± 1.7*	-
		mRNA vaccine	*Dhaliwal et al.* [134]	*195.05 ± 4.5*	*0.19 ± 0.02*	*+ 35.6 ± 3.0*	*80.0 ± 5.0*	-
	Cubosomes	Saquinavir-Anti-HIV	*Hosny et al.* [135]	*120 ± 2*	-	-	*72 ± 1*	-
		Rosuvastatin-Epilespy	*Ahmed et al.* [136]	*219.15 ± 8.14*	*0.240 ± 0.03*	*- 26.2*	*70.30 ± 1.84*	-

doi: 10.1016/j.addr.2021.113826

		Donepezil-Alzheimer's disease	*Patil et al.* [74]	*143.6*	*0.38*	*Above - 40*	*48.48 ± 0.32*	-
Hybrid systems	Cyclodextrin, liposome	Butylidenephthalide-Anticancer	*Lin et al.* [84]	*253.0 ± 6.05*	*0.33 ± 0.01*	-	*58.2 ± 2.3*	*18*
	Chitosan, anionic liposome	Sumatriptan-Migraine	*Assadpour et al.* [73]	*167.33 ± 3.39*	*0.20 ± 0.06*	*- 35.25 ± 0.02*	*21.5 ± 0.2*	-
	Chitosan, anionic liposome	Ghrelin-Cachexia	*Salade et al.* [31]	*263 ± 5*	*0.203*	*+ 9 ± 1.2*	*64 ± 2*	-

• Devices

After developing the formulation, device selection to deliver the formulation is crucial to develop an effective final product (Figure 1.2).

Although such selection may appear marginal compared to the pre-formulation step, the device influences the plume geometry, the size and the velocity of the particles. All these parameters greatly impact delivery efficiency. Moreover, those parameters not only depend on the device itself but also the drug properties. This coupling between formulation and devices shows the importance of considering the formulation strategy as a whole and not in distinct parts. In this section, we briefly report the devices used for liquid formulations and as well as dry powders and explain their influence on the deposition.

○ Liquid formulation

The most described devices for liquid drugs delivery are sprays. These devices create a liquid cone that breaks up [137–139], or a Taylor cone in the case of electrosprays [140,141], forming droplets with a mean aerodynamic diameter ranging from 10 to 50µm [142] and from 100 nm to 50 µm for electrosprays [143] (Figure 10). The most widespread spray models are spray pump, but for high-value drugs, such as vaccines or neurologic medicines, single or dual-dose devices are preferred. Some examples of these emerging apparatuses are Aptar Unidose (UDS) and Bidose (BDS) Systems [144], or Mystic Pharmaceutical VeriDoser® [145] that are all devised for reaching the olfactory region. Most interestingly, they are all available to deliver dried powder formulations.

In addition to the sprays, nebulisers may also be used to reach the olfactory mucosa. They are based on vibrating mesh, ultrasounds or liquid jet to nebulize the liquid dispersion [26,146].

doi: 10.1016/j.addr.2021.113826

All of them produce smaller droplets characterized by a mean aerodynamic diameter ranging from 1 to 5 µm and a velocity from 1 to 3 m/s [142,147] (Figure 10). The small size of the generated particles can be a problem since they can enter the lower respiratory tract [142]. However, particular models have been developed to target the olfactory zone without disseminating droplets in the whole cavity, which lead to the inhalation of the smallest ones. Examples of these specialized nebulisers include the Kurve Technology ViaNase™ atomiser [148] (Figure 11a) or Impel NeuroPharma Precision Olfactory Delivery (POD®) device [149], the latter existing also for powder delivery.

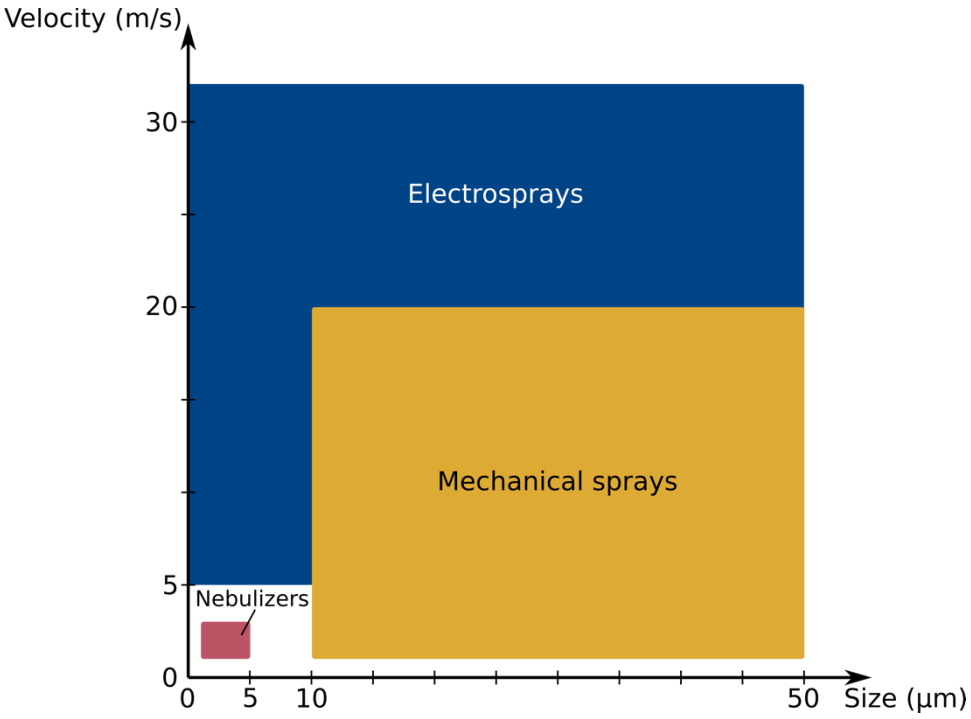

Figure 10: The regions represent the velocity and particle size that can be achieved by nebulizers (red, on the left), mechanical sprays (yellow, on the right) and electrosprays (blue, in the background). The exact range can be smaller depending of the device model and the formulation.

○ Dried powder formulations

Similarly to liquid formulations, sprays are usually used to deliver dried powder formulation to the olfactory region. They rely on compressed air or another inert gas to propel the particles into the nostrils with a velocity ranging from 1 to 20 m/s [94,137,142,150]. The most described devices are Aptar® UDS and BDS [31], which are specially designed for N2B, or Shin Nippon Biomedical Laboratories Fit-lizer™ (Figure 11b)

doi: 10.1016/j.addr.2021.113826

Other technologies for powder delivery have been developed based on the breathing out of the patient. These platforms take advantage of the soft palate raise during a forced expiration by the mouth [151] . The general principle is to blow in a pipe connecting the mouth and the nose and containing the drug-loaded formulation [152]. In this manner, the expired air carries away the powder from the device to the nose. Therefore, there is no deposition past the nasopharynx, even for particles with a mean aerodynamic diameter lower than 5 µm [152]. The deposition pattern of insufflators differs from other devices. *Xi et al.* observed a mean increase by a factor of 2.75 for the deposition in the whole nose and 1.35 in the olfactory region compared to classical nebulizers. *Djupesland and Skretting* compared an insufflator and reported a 7-fold increase in the deposit in the upper posterior zone while decreasing by a factor of 5 the deposition in the lower posterior region [26,153]. Examples of this kind of devices are the Optinose™ Exhalation Delivery System (EDS) [151] (Figure 11c), which also exists in a liquid version, or the IP Med TriVair™ device [152] (Figure 11d).

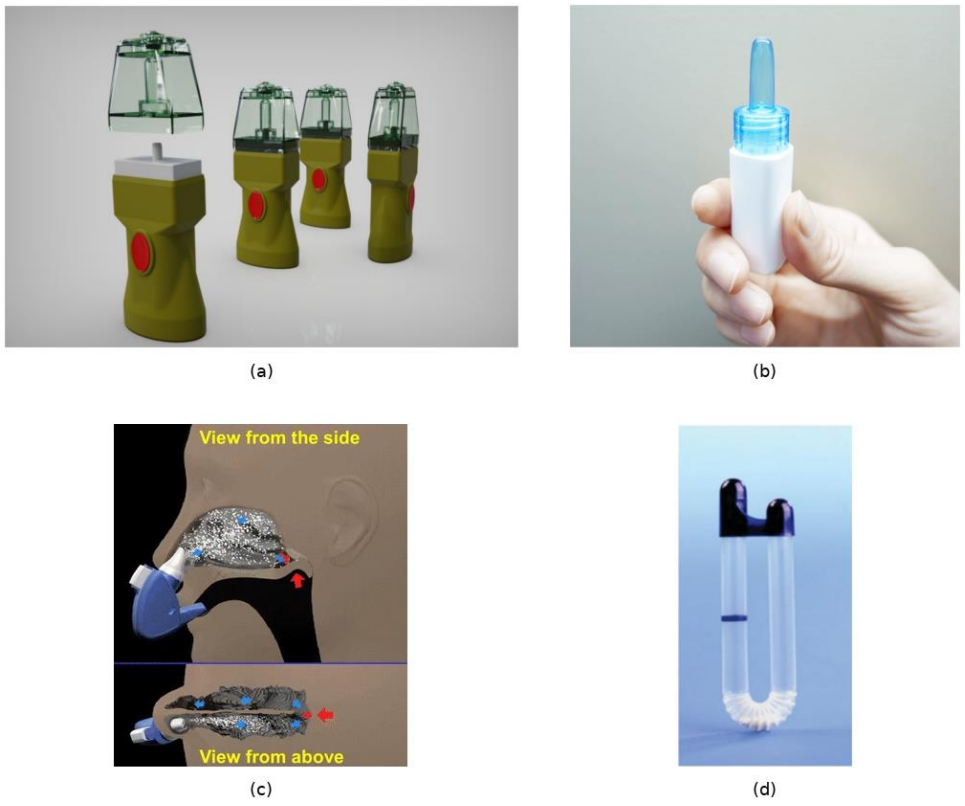

Figure 11: Various Nasal devices. *(a)* ViaNase™ atomiser. Image by Kurve Technology, Inc. Reproduced with permission. (b) Fit-Lizer™ technology. Image by Shin Nippon Biomedical Laboratories. Reproduced with permission. (c) Optinose™ sytem. Reproduced with permission from [151]. Copyright 2013 Springer Science Business Media New York. (d) TriVair™ insufflator [152] . Copyright 2013 John Wiley and Sons.

doi: 10.1016/j.addr.2021.113826

Influence on the drug delivery

The plume geometry, and more precisely its opening angle, is of crucial importance for N2B drug delivery. Indeed, devices with a smaller plume angle better penetrate past the nasal valve thanks to lower impaction [22,88,89,154]. *Moraga-Espinoza et al.* showed that decreasing the plume angle from 46° to 37° and 25° increased the deposition past the nasal valve from around 40% to respectively about 55% and 85% [88]. Similarly, *Pu et al.* observed an increase in the turbinate deposition from approximately 30% to 55% and the plume angle decreasing from 50° to 37° [89]. *Foo et al.* reported the same trend, with narrower spray penetrating further in the cavities but also noted that the wider spray deposited lower in the nose, with a decrease in the portion in upper turbinates plunging from about 20% to nearly no deposition [154]. Finally, *Sawant et al.* also reported that narrow sprays deposit further in paediatric casts but most importantly showed that classic device-formulation combinations do not cross the nasal valve in children [90], underlining the importance of pre-formulation for particular groups.

Inthavong et al. have also demonstrated that sprays generating smaller plume diameters or hollow cones were more efficient to better penetrate the cavities [137].

Second, particles size is limited by two factors. First, they have to be bigger than 5µm (and preferably 10 µm) to avoid lung deposition [142]. Moreover, their diameter should be between 8 to 12 µm, which is optimum to reach the olfactory zone. If the particle diameter is larger than 12 µm, they mostly impact the nasal vestibule walls [94,137,155]. If it is smaller than 8 µm, they follow the streamlines in the lower and middle turbinates instead of going up to the olfactory region [94,155]. The size of liquid droplets depends on the device and the rheological properties of the spray [22,24,25]. Similarly, powder granulometry is also determined by the formulation but changes when used in an administration device [156,157].

As already mentioned, bigger particles are more retained in the nasal vestibule. But the relevant parameter is not particle diameter but their kinetic energy. Fast, massive particles stay in the anterior part of the nose. On the other hand, small and slower particles pass in the turbinates more easily [94,155]. It worth noting that, for liquid spray, the liquid swirls when being discharged. A significant part of the velocity can thus be tangential. A high-vorticity cone permits more passage to the posterior turbinates but also the nasopharynx [137].

Development and use of 3D-printed nasal casts

doi: 10.1016/j.addr.2021.113826

Pre-formulation studies ensure that the nasal products have suitable characteristics. However, those are *a priori* tests. One way to evaluate these formulations is the use of 3D-printed nasal casts. They allow testing the efficiency of nasal products in a more realistic way than standard tests while being cheaper and easier than clinical trials. They permit to verify if the particle size distribution is suitable for N2B administration and/or if the device is appropriate. However, it is necessary to mention that experiments in nasal casts are restricted to the evaluation of the transport of the formulation from the instillation device to the olfactory zone (Figure 1.3) but does not provide information about the diffusion through nasal mucosa as well as the bioavailability of the drug in the brain.

The survey of the literature shows that the following four steps are usually adopted to prepare the experimental campaign with a nasal cast:

- Outline the general shape of the study by taking into account the constraints;
- Adapt the design to the objective of the study;
- Choose the 3D printer adapted to the needs;
- Decide the type of mucus to add into the cast

Accordingly, the structure of this section is organized into four corresponding sub-sections.

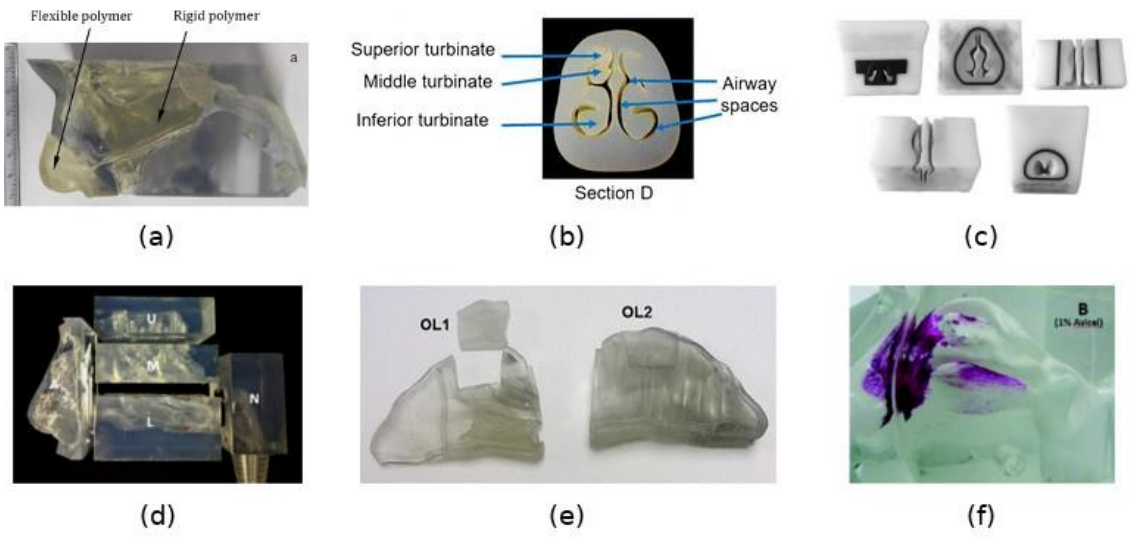

Figure 12: Diverse nasal cast models. (a) Adapted with permission from [158] Copyright 2020 Elsevier. (b) Reproduced with permission from [90] Copyright 2018 Springer Science Business Media New York. (c) Adapted with permission from [25] Copyright 2019 Elsevier. (d) Adapted with permission from [24] Copyright 2018 American Chemical Society. (e) Adapted with permission from [146] Copyright 2016 Springer Science Business Media New York. (f) Adapted with permission from [89] Copyright 2014 Taylor & Francis.

doi: 10.1016/j.addr.2021.113826

○ Constraints integration

Nasal casts can differ in their external shape (e.g. wide block or thin walls), materials or sections (e.g. following an anatomical plane or not). Those characteristics depend on the scope of the study but also its implementation. Therefore, it seems relevant to list the constraints linked to the type of measures and the experiment design. In this way, the general characteristics of the cast before its conception may be outlined.

After the formulation instillation in the nasal cast, quantification of the drug is performed to evaluate its distribution throughout the different cavities. Indeed, as mentioned in the introduction, when a N2B delivery is wanted, drug deposition should be maximal in the olfactory region. However, such evaluations are usually not so simple as the nasal cast should be resistant to various constraints linked to the appropriate analytical methods.

The first category of evaluations consists of recovering the active ingredient. It is usually done by rinsing the cast with a suitable solvent, which should dissolve the formulation (or at least the drug) without alteration of the cast material. Analysis of washing liquid, using spectroscopy [22,24,88,154], HPLC [21,23,25] but also other techniques [156,157,159], follows the rinsing step to determine the spray deposition through the cavities. The casts used with this method are cut to have the best information according to the scope of the study. *Sawant et al.* divided their cast into vertical slices to assess how far the spay penetrates in the nose (Figure 12b) [90]. Contrary to the previous team, *Wingrove et al.* (Figure 12c) and *Warnken et al.* (Figure 12d) adopted a partition consisting of five pieces: one for the nostrils, one for the pharynx and one for each turbinate (lower, middle and upper) [24,25]. This allows measuring the vertical distribution of the spray, a crucial piece of information for N2B delivery. Note that the cast used by *Wingrove et al.* is equipped with seals to ensure no leaks between the parts.

A second technique consists of weighting the different parts of the cast. This second method requires precision of the order of 1mg. Therefore, replicas intended for weighting are lighter to comply with the scale capacity [26,146]. For example, the nasal cast produced by *Xi et al.* [146] has one piece for each side of the nose, with a detachable part for the olfactory region, and two more pieces for the nostrils and the nasopharynx, which are assembled by grooves (Figure 12e). This assembly, combined with fine walls, reduces the mass of each part (since no external fixation is needed) and permits to only weigh the pieces of interest.

doi: 10.1016/j.addr.2021.113826

For both types of evaluations, the crucial information is the percentage of the formulation that reaches the olfactory region. However, it can be beneficial to have multiple cast pieces instead of a single measure in the olfactory zone [21,24,25,88,157]. In this way, the sum of all recovered quantities and the drug remaining in the device should be equal to the total amount of formulation instilled in the cast. In the end, such a procedure provides an estimation of the efficiency of the recovery process.

The recovery rate can be altered by the potential porosity of the cast, especially for parts printed using fused deposition modelling [160] or powder-bed fusion [161]. Also, if the *in vitro* evaluations are performed simultaneously with a simulation procedure [11,26], multiple quantification points enable researchers to build more confidence in the simulation results. Nevertheless, the more parts the cast have, the longer the analysis procedure will be. Therefore, the number of parts inherent to the cast is a trade-off between precision and efficiency. In addition to the number of parts, the cutting of the nose into pieces is also relevant. For N2B delivery, having a section dedicated to the olfactory is mandatory. The rest of the parts can be coronal cuts to evaluate the penetration depth of particles inside the cavities or horizontal cuts to quantify how the spray distributes vertically and, so, which are the obstacles hindering olfactory zone targeting.

The quantification of liquid spray distribution can also be done using colorimetric gels (e.g. Sar-Gel®, Kolor-Kut®). Those substances are coated inside the cast and change colouration when exposed to humidity. The colour intensity provides information about the amount of spray that is deposited across the cast [26,89,146,162]. Thus, it is necessary to have transparent materials and fine walls in contrast with block-like replicas. For instance, the cast made by *Sosnowski et al.* has four pieces corresponding to the nostrils, the septum and each side of the nose (Figure 12a) [158]. With this cutting, it is thus possible to have a quasi-direct view on each portion of the cast to measure optically the aerosol deposition. Another cast described before, made by *Xi et al.,* has fine walls to allow weighting [146]. So, it is also adapted for optical measurements if the material used is transparent (Figure 12e). Another solution, used by *Pu et al.* is to work with a silicone transparent commercial cast made by Koken and intended for education (Figure 12f) [89].

Finally, a last type of measures implies spraying a radiolabelled drug in the cast. The deposition pattern comes out from the radiation intensity evaluation in each zone [93]. The big restriction here is not to use materials that would absorb the radiations as metal. Note that cast design should also limit the exposition to radiation inherent to this procedure.

doi: 10.1016/j.addr.2021.113826

Study-centred design

A realistic cast guarantees to be very close to the anatomy of a patient. However, it does not assure a successful deposition study. Moreover, some production facilitations might occur without affecting the results. Finally, having a perfect representation of an individual nasal cavity does not give any information about the general population. For those reasons, researchers should identify their goals to develop a suitable 3D printed nasal cast.

Realism of the cast

Accurate reproduction of actual nasal cavities is often suitable to study spray deposition. However, in some cases, researchers are interested in exploring how particular features impact nasal drug delivery. In this case, an appropriate method is to modify the numerical models to see how the alterations influence the airflow [163,164]. Researchers could predict the efficiency of drug delivery in patients, knowing their nose geometry characteristics.
A more radical approach is to create ideal geometry to provide a standard test apparatus for N2B delivery [94,155,165]. Therefore, it seems that the main challenge in developing 3D nasal casts is to manage the opposition between personalisation and norm creation.
Finally, another element to take into consideration is the easiness of production. For instance, the sinuses presence is not significant when developing a 3D printed nasal cast intending for N2B delivery. Indeed, researchers have shown that their influence on airflow in healthy patients is negligible [163,164,166,167]. Consequently, it seems that sinuses can be erased from the final cast without changing the global distribution of the formulation. The main advantage of such adaptation is the reduction of printing time and easiness of the design.

Standard and individual cast

Some research teams may want to design patient-specific treatments [24,139]. On the other hand, some groups may want to evaluate the deposition of a formulation in the whole population at the early stage of the development (preformulation step) [21,165]. These two approaches would lead to the development of different casts.
When targeting individual medicine, the 3D replica should be as close as possible to the patient cavities. Such aims may be interesting for patients who present nasal pathologies as a septal deviation. Indeed, a septal deviation is reported to dramatically changes the airflow inside the turbinates [20,168] as well as the particle trajectories [20,168]. It is also attractive for older patients as the anatomy of the nostrils may be modified through the ages [169].

doi: 10.1016/j.addr.2021.113826

In contrast, if the goal is to obtain a formulation for a broad range of the population, two possibilities exist. The first one is to use multiple casts with the same administration strategy and find a procedure that would fit all of them [24].
The other possibility is to create a median cast, or even an idealised cast, that would represent the population of interest [94,165,170]. But this last approach does not imply taking into account the broadest possible range of people. Indeed, as stated earlier, older patients have specific pathologies. Therefore, a distinct cast could be suitable.
Similarly, paediatric patients would require a specific test bench. Indeed, *Sawant et al.* Reported that the small dimensions of their airways impose appropriate strategies [22] (Figure 12a and b). But through the conception of a general cast, it is crucial to stay representative of the target group. For instance, *Keeler et al.* showed that different ethnic groups have different medians anatomies which result in different deposition patterns [167].

○ Choice of the 3D-printing technique for nasal cast

As already mentioned, creating a suitable 3D-printed nasal cast is a prerequisite to perform a conclusive *in vitro* evaluation of a nasal formulation intended for N2B delivery. However, the transition between numerical and physical models can also influence the fidelity of *in vitro* geometries. Therefore, the choice of an adapted 3D printing technology seems to be crucial for efficacious *in vitro* experiments. The main characteristics of 3D-printing technologies relevant for nasal cast production are presented in this section (Table 4). The companion question of coating this cast with artificial mucus will be addressed in Section 4.4.

▪ *Comparison of 3D-printing technologies for nasal cast*

Fused deposition modelling

Fused deposition modelling (FDM) is the most widespread 3D printing technology because of its low cost and ease of use [171,172]. This technology warms thermoplastic filaments above their melting point and extrudes them via two rollers. The molten material is deposited in a thin layer (**Erreur ! Source du renvoi introuvable.**). Next, the build plate is lowered to gradually build 3D pieces [172,173]. The choice of materials available to use in those 3D printers is limited to thermoplastic compounds, despite noteworthy advances in their diversity (e.g. transparent or flexible filaments) [171].
The central element of FDM is the way the layers are formed. In particular, extrusion does not allow tiny layers creation causing a limited vertical resolution [174,175]. Indeed, if the layer

doi: 10.1016/j.addr.2021.113826

height is too large compared to the nozzle diameter, the fused material breaks and does not adhere to the previous layer or the build plate [176]. *Löffler and Koch* report a typical layer thickness of 0.1 mm for a 0.2 mm nozzle and 0.5 mm for a 1 mm nozzle [176]. Moreover, it creates rather large steps that will result in a rough surface state [174,175]. Also, most thermoplastic materials experience some thermal shrinkage, i.e. the retraction of plastic due to a temperature drop, which can reduce the precision of the print [174,177]. These effects lead to an overall accuracy of about 100 to 150 µm [178,179]. This precision can be problematic in studies researching optimum patient-specific configuration. Indeed, the allowed uncertainty on parameters is minute [94]. For example, *Warnken et al.* determined the spray insertion angle within a tenth of a degree [24]. High precision is thus advised to get the exact values for those parameters.

Thermal shrinkage can also be responsible for the delamination phenomenon, i.e. layers detaching from each other [174,177,180]. It happens if the bond between them is too weak because of insufficient layer adhesion or high thermal stress for the material [177]. Delamination creates holes in the final piece and makes it porous [181]. Finally, the resistance to organic and inorganic solvents varies with the plastic used to print the cast [180]. Solvents used for drug recovery include water, ethanol, alkaline solutions, acetic acid, dimethylformamide or dichloromethane (Table 3). It appears from this data that polypropylene has the highest resistance of solvent and should be the most suitable polymer to build nasal casts. On the other hand, if the studied drug is recovered using water or ethanol, nearly all commercial filaments can be used.

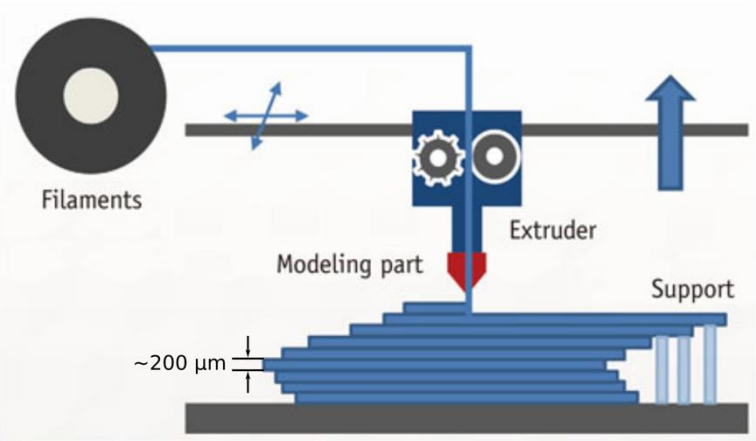

Figure 13: Principle of fused deposition modelling. Reproduced with permission from [175].

Table 3: Thermoplastic resistance to solvents: (+++) stable (+) moderately stable, (-) unstable. Data from Erokhin et al. [180]

doi: 10.1016/j.addr.2021.113826

	Water	Ethanol	NaOH solution	Acetic Acid	Ethyl Acetate	Dimethyl-formamide	Dichloro-methane
ABS	+++	+++	+++	+++	-	+	-
PLA	+++	+++	+++	+++	-	+	-
HIPS	+++	+++	+++	+++	-	+	-
PETG	+++	+++	+++	+++	++	+	-
PP	+++	+++	+++	+++	+++	+++	+++

Stereolithography

Stereolithography (SLA) builds 3D objects by shining UV light on the top of a tank filled with photosensitive resin. When illuminated, the first micrometres of resin harden and bind to the previously fabricated layers or the build plate (**Erreur ! Source du renvoi introuvable.**). The plate is then lowered so that a film of resin covers the object and a new layer can be deposited [173,174,182]. Moreover, pieces produced with this method require post-processing to remove all non-cured resin from the final part to avoid leaches in subsequent experiments [21].

Since this method does not imply heating, thermal shrinkage is a lesser issue. Therefore, the print precision is only constrained by the layer height and the resolution of the light source. Moreover, the minimum layer height is far smaller than extrusion-based processes (around 25 µm instead of 100 µm) [175,183]. It induces a far greater ultimate precision of roughly 30 to 50 µm [179,184]. Moreover, by using smaller layers, this technique can produce a far better surface finish than FDM [174,175] (Figure 12d). Post-processing is required to remove the remaining non-cured material of the part [175] that would otherwise contaminate rinsing liquid [21]. Even with a thorough washing procedure, the printed pieces can be altered by solvents. *Kotz et al.* demonstrated that samples printed with Formlabs Though resin gain weight when plunged in methanol, dichloromethane, tetrahydrofuran or acetone, indicating an incompatibility with these chemicals [185]. On the other hand, the pH resistance of classical resin is great. For instance, *Kletetschka et al.* reported that the Formlabs Standard Clear resin is almost not altered if they are immersed for 18 days in solutions with pH ranging from 0 to 12 [186]. Another limitation of SLA is the relatively small range of resins available. While they can provide good transparency, the pieces produced are often brittle [175]. On the other hand, the use of resin instead of thermoplastics results in non-porous parts [187], as shown by the 100% recovery rate obtained by teams using SLA casts [88,124,183]. These parts are also not subject to delamination.

doi: 10.1016/j.addr.2021.113826

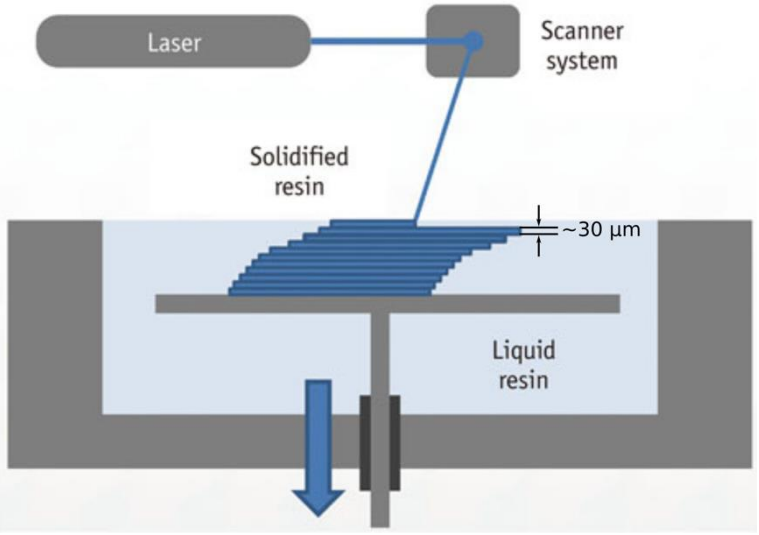

Figure 14: Principle of stereolithography. Reproduced with permission from [175].

Powder-bed Fusion

Powder-bed fusion processes are known as Selective Laser Sintering (SLS), Selective Laser Melting (SLM) or Electron Beam Melting (EBM) [21,171,174,175,182]. The powder used in the process can be metallic or polymeric. The energy source heats the powder bed until particles are partially (sintering) or totally (melting) fused (**Erreur ! Source du renvoi introuvable.**). Then, a new blanket of powder is put on the top and then melted again on the piece [171,174,175,182]. Excluding the expensive equipment, printing is not too costly since this technique can process multiple parts at once [21].

The precision of such machines is as good as SLA printers [174,175]. Indeed, they both rely on a laser spot to produce the objects. But contrary to SLA printers, powder bed printers induces much thermal stress [174]. So, precision is a bit less: about 40 to 50 µm [179,188]. The use of powder instead of resin also prevents any leak after the printing [21,189]. The material should still not dissolve in the employed solvent. For instance, PLA can be used in SLS [190] and is degraded in organic solvents such as acetone or dichloromethane [180]. Nylon is also extensively used in SLS [190] and is stable in the vast majority of solvents [21,180]. Therefore, nylon has been used to create nasal casts [21,23,93]. However, powder beds have two disadvantages over resin-based 3D printing methods. Indeed, a perfect melting of particles is very difficult to obtain. The final structure is almost always porous [21,171,174]. Moreover, imperfect melting also leads to an abrasive surface [21]. It worth noting that the size of polymer particles is usually smaller than the metallic ones. The surface state is thus usually smoother for plastic parts compared to metal [21].

doi: 10.1016/j.addr.2021.113826

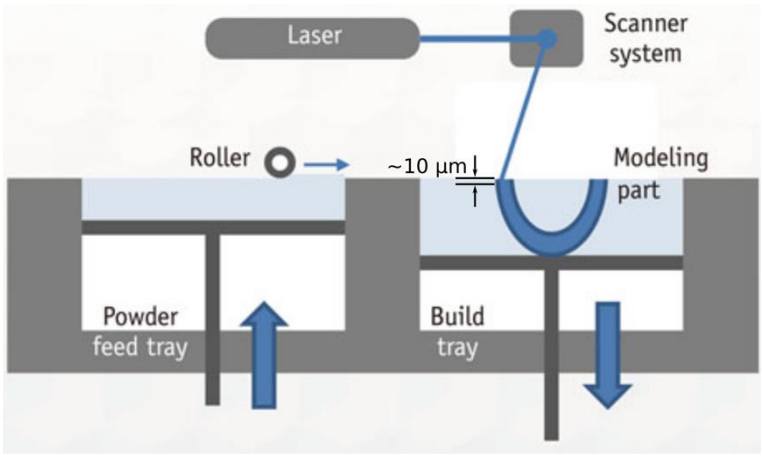

Figure 15: Principle of selective laser sintering. Reproduced with permission from [175].

Material Jetting

The principle of material jetting is to deposit droplets of UV sensitive resin layer by layer. The drops are immediately hardened with a lamp to create a 3D geometry [171,174,175,182]. The system usually consists of two printing heads: one for the printing material itself and one for support material which is removed during post-processing treatment [171,175,191] (**Erreur ! Source du renvoi introuvable.**). Other names of this technique are MultiJet or PolyJet Printing [175], the latter being a Stratasys trademark. The variety of available materials is ample, offering transparent or opaque and rigid or soft materials [171,174,175,182]. Soft materials are often used for nostrils productions to better insert the device [158] (Figure 12a). Some casts are even entirely printed in soft polymer to reproduce better the compliance of natural tissues [90] (Figure 12b). On the other hand, transparent plastics must be used if the procedure implies an optical measure of the deposition [26,146]. However, this technology is more expensive and requires time-consuming post-processing [175].

The layers formed by fine droplets are only about 15 µm high [175]. Consequently, the surface finish is very smooth [146,174,175], like their precision (from 25 to 40 µm) [179,192] (Figure 12a, b, c and e). However, the materials employed usually deform easily if warmed, even at a moderate temperature [175]. The objects are not porous even though *Chen et al.* reported pharmaceutical ingredients infiltrations in the cast made with VeroGray RGD850 [165]. The problem was solved using nail polish to coat the interior of the replica. The inverse also true: the support material is not completely removed and is prone to contaminating measures. Therefore, a thorough cleaning procedure should be carried out to avoid this issue [191].

doi: 10.1016/j.addr.2021.113826

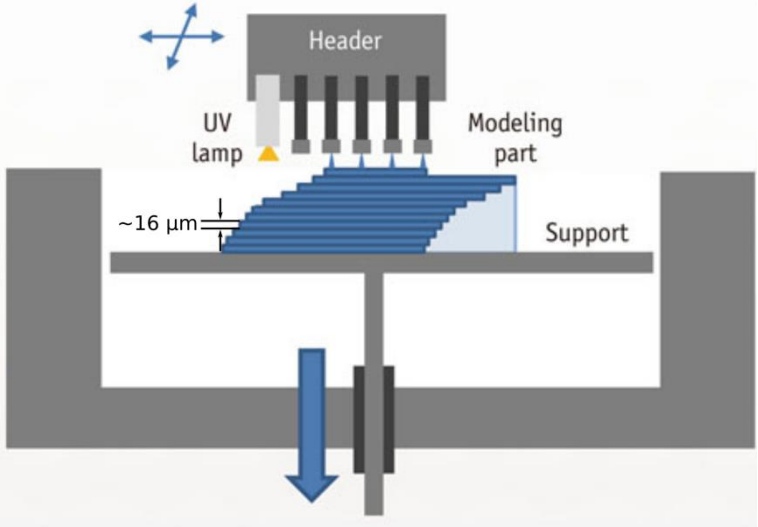

Figure 16: Principle of PolyJet. Adapted with permission from [175].

Table 4: Key characteristics of 3D printing technologies.

Printing technique	**Surface finish**	**Precision**	**Porosity**	**Material contamination**
Fused Deposition Modelling [174,175,180]	--	--	- Delamination	- Depends on material
Stereolithography [174,175,180]	++	++	No	- Depends on material
Powder-bed Fusion [21,174,175,189]	-	++	Yes	No
Material Jetting [146,165,174,175,191]	++	+	Low	Yes

- *Relevant characteristics for cast production*

Surface state

doi: 10.1016/j.addr.2021.113826

A problem inherent to all additive manufacturing techniques is artificial roughness [171,174,182]. Indeed, objects are created by putting layers of materials on top of each other. Consequently, to build a 3D curve, successive layers have slightly different shapes. Therefore, the transition between them is not smooth but stair-like [171,174,175]. The bigger the layers are, the rougher the surface will be.

On the other hand, mucus covers the surface of nasal cavities and smooths them [193]. Therefore, it seems mandatory to decrease the manufacturing roughness to better mimic nasal cavities. This aspect is especially relevant if the study implies generating air flux inside the nose. Indeed, an unnatural surface finish can create more turbulence and therefore affect the airflow in the cast [194]. In particular, *Schroeter et al.* demonstrated that 10µm and 20µm particles are mostly deposited in anterior parts of the nose and closer to the nasal floor if the roughness increases. They also showed that 10 µm particles better penetrate the nasopharynx in smoother casts [194].

Also, the surface finish can influence the resistance encountered by airflow in the cast. The more rough the walls are, the higher the pressure drop across the cavity will be [194]. However, it should be noted that individual variation also drastically influences the pressure drop: *Chen et al.* Measured, for an airflow of 20L/min, drops ranging from 5 to 20 Pa in different cast using the same printing procedure and thus having similar roughness [195].

Precision

As stated earlier, having a replica geometry as close as possible to *in vivo* geometry may be wanted by research teams. Therefore, the accuracy of the 3D printer is a fundamental issue in the choice of one technology instead of another.

Indeed, the resolution of the 3D printer [171,174,175,182] limits the precision of the final object. A more precise machine can print finer details and reproduce with more details the actual anatomy. For N2B delivery, a more accurate printer better recreates the olfactory cleft, which is around 2 mm wide [196]. Therefore, realistic results are expected. Up to now, no study compared the same drug administration in casts printed by different techniques.

The similarity between actual and artificial cavities is also affected by the deformations that may occur in the time between printing and experiments. These deformations may appear from thermal stresses [171,174,182] or inadequate procedures which may include the heating of the piece to temperatures that cause the material to soften or exposure to excessive mechanical stress [175]. For instance, some resins can deform easily if warmed in an oven for drying [197].

Porosity

doi: 10.1016/j.addr.2021.113826

Most of the *in vitro* studies evaluate the spatial distribution of the formulation by disassembling the replica and rinsing each piece with a solvent to recover the active ingredient [11,21–25,31,88,154,157]. However, if the cast absorbs a part of the formulation, the detected amount of drug will not correspond to the actual quantity of drug deposited onto the pieces. *Hughes et al.* reported recovery rates as low as 20% for a stainless steel cast [21]. Therefore, studies implying a washing step should not use a porous cast.

The principal source of porosity seems to be the intrinsic porosity of the material [21]. But cast porosity can also be caused by tiny holes appearing between the print layers, during the printing or the post-processing step [177,180].

Material contamination

Like porosity, cast material leak is a problem for casts if they are rinsed to quantify drug deposit. Indeed, cast material in the analysed washing liquid can interfere with spectroscopic or chromatographic measure and hinder the deposition evaluation. Such issues have been reported by *Hughes et al.* during preliminary studies[21].

Contamination primary comes from the cast material itself [21,180] but can also arise from the support material used by the 3D printer [191]. It highlights the importance of considering not only the cast material itself but also the potential support material. Therefore, careful support removal and appropriate washing procedure should precede before the first recovery tests.

The main problem is the overlapping between the absorption spectrum of the material and the API that must be retrieved [198]. Consequently, the quantification of drug distribution would require looking for non-overlapping peaks, which can be challenging if the material absorbs a broad range of wavelengths (e.g. some photopolymer resins in the UV spectrum) [191]. Given that SLA and material jetting resins are made to absorb UV light, one solution can be changing from ultraviolet to infrared spectroscopy, but the resin absorption spectrum is still nonzero [198]. Finally, let us mention that extrusion-based materials are also detectable by spectroscopy and so can also interfere with the measurements [199,200].

- *Cast comparison*

This section aims to compare different nasal cast to outline their advantages and drawbacks.

Table 5: Nasal casts produced with different technologies.

Used techology	Research teams	Cast details	Experiments performed

doi: 10.1016/j.addr.2021.113826

Fused Deposition Modelling	*Le Guellec et al.* [201]	• Made of ABS • Based on CT-scans	• Nebulisation of radiolabelled droplets • Replica not accurate enough to reproduce *in-vivo* deposition
Stereolithography	*Kelly et al.* [183]	• Manufactured using SLA 7000 and Viper™ Si2 machines • Based on MRI-scans	• Ethanol-DEHS aerosols (diameter from 1 to 10 µm) • Roughness and inaccuracy of the cast influence the deposition
	Moraga-Espinosa et al. [88]	• Manufactured using Viper™ HA SLA systems with Somos® Watershed XC 11122 • Casts based on CT-scans • Divided into five parts (nasal valve, lower, middle and upper turbinates and nasopharynx)	• Liquid sprays of cromolyn sodium solution • Turbinate deposition mainly influenced by spray geometry
	Sartoretti et al. [202]	• Made of epoxy resin • Nostrils made of silicone • Based on a 33-year-old female cadaver without nasal disease	• Liquid spray of iodine-labelled solutions • Proof of concept for the measurement method
	Schoeter et al. [11]	• Based on MRI-scans of a healthy non-smoking adult male • Geometry identical to Kelly et al.[183] • Divided in six regions (nasal vestibule, nasal valve, anterior turbinates, olfactory region, turbinates and nasopharynx)	• Ammonium fluorescein aerosols (2.6 to 14.3 µm) • Optimum range for deposition in central regions: 10-11 µm • Deposition of particles with size >12 µm mainly in the vestibule • Deposition in the cast in accordance with CFD simulations

doi: 10.1016/j.addr.2021.113826

	Warnken et al. [24]	• Manufactured using a Viper™ HA SLA system with Watershed XC 11122 • Multiple casts based on adult and paediatric CT-scans • Divided in five parts (vestibule, nasopharynx and upper, lower and middle turbinates)	• Liquid sprays of cromolyn sodium solution • Improvement of turbinate deposition if patient-specific angle is used • No significant effect of the inspiration and plume angle on deposition
Selective laser sintering	*Hughes et al.* [21]	• Made of Duraform PA nylon • Based on healthy female CT-scans	• Liquid spray • Majority of the dose delivered in the nostrils and the nasal valve • Small differences between the two anatomies • Significant effect of the angle and position of the spray nozzle
	Shah et al. [23,93]	• Made of Duraform PA nylon • Based on CT-scans • Divided in five sections (nasal vestibule and valve, front turbinates, rear turbinates, olfactory region and nasopharynx)	• Liquid spray of radiolabelled mometasone furoate formulation • Majority of the dose deposited in the turbinates region • Matching depositions *in vitro* and *in vivo*
PolyJet	*Chen et al.* [165]	• Manufactured using Objet Eden 350 V High Resolution 3D Printer with Objet VeroGray RGD850 resin • Idealised geomotry based on 12 CT-scans	• Cromolyn sodium spray pumps • Deposition in idealised geometry corresponding to average deposition in real anatomies

doi: 10.1016/j.addr.2021.113826

	Sawant et al. [90]	• Manufactured using Object Eden 350 3D printer using Durus White Photopolymer • Based on MRI of 12-years-old child • Divided in five sections (nasal vestibule, nasal valve, front and rear turbinates and nasopharynx)	• Liquid sprays of glycerian/water mixture labelled with Aniline Blue • Significant differences between adult and paediatric casts • Anterior deposition increased in child cavities
	Trows et al. [156]	• Divided in five segments (nostrils, nasal vestibule, lower, middle and upper turbinates and nasopharynx)	• Dry spray of chitosan particles • Inhaled fraction higher for smaller particles • High proportion of the drug deposited in the nasal vestibule
	Wingrove et al. [25]	• Based on adult CT-scan	• Liquid spray of insulin solution • Influence of the administration device on the deposition pattern • Deposition of larger droplets mainly in the vestibule • Narrow plumes not-suitable for nose-to-brain delivery • Correlation between *in vitro* and *in vivo* tests
	Xi et al. [146,203]	• Manufactured using Stratasys Objet30 Pro with Veroclear polypropylene • Based on a CT-scan of a 53-year-old male • Divided in six parts (nostrils, nasopharynx, left and right cavities, left and right olfactory zone)	• Classical and bi-directional nebulisers • Bi-directional systems producing smaller droplets more efficient to reach to olfactory area
Milling	*Cheng et al.* [159]	• Formed of 77, 1.5 mm thick, acrylic sheets	• Uranine-labelled di(2-ethylhexyl) sebacate

doi: 10.1016/j.addr.2021.113826

		• Based on MRI of 53-year-old non-smoking Caucasian male	aerosols (size of 1 to 9 µm) • Spray of ^{3}H-radiolabelled suspension • Small post-nasal fraction for sprays • Droplet size influenced by the instillation device • Increased anterior deposition for larger droplets are wider plume angles
	Foo et al. [154]	• Composed of 72, 1.5 mm thick, acrylic sheets • Based on MRI of 53-year-old healthy Caucasian male	• Sprays using mixtures of methanol, ethanol, glycerine and rhodamine 590 tetrafluoroborate • Better penetration in the turbinates for smaller plume angles • Little effect of the droplet size
	Häußermann et al. [204]	• Based on MRI of 50-year-old Caucasian male	• Monodisperse sebacate oil droplets aerosol (diameters from 1.7 to 10 µm) • Deposition significantly higher under constant flow compared to human breathing
Koken Cast	*Kundoor et al.* [205]	• Made of transparent silicone	• Commercial liquid sprays (Ayr Saline Nasal Gel No-Drip Sinus Spray, Afrin No Drip Original 12 h Pump Mist, and Zicam No-Drip Liquid Nasal Gel Non-Drowsy Seasonal Allergy Relief)

doi: 10.1016/j.addr.2021.113826

		• Spray insertion angle and head tilt angle more important than insertion depth. • More viscous sprays associated to smaller turbinate coverage
	Lungare et al. [162]	• Adamantine thermoresponsive hydrogel-based spray • Increased deposition in the vestibule for more vertical instillations • Forward head-tilting leading to more depition in middle and upper turbinates • Less dispersed deposition patterns for more viscous sprays
	Pu et al. [89]	• Liquid spray using mometasone furoate solutions • Higher viscosity correlated with lesser anterior deposition • Deposition pattern and dripping influenced by rheological properties of the spray

Very few casts have been produced using fused deposition modelling [27] (Table 5). It can be explained by the poor resolution and surface finish offered by this technique. Indeed, Le Gellec et al. demonstrated that the aerosol pattern in their FDM replica is different from the corresponding plastinated cast (preserved cadaver head) and *in vivo* results due to the rough surface state.

The three most commonly used 3D printing techniques (SLA [11,24,88,183,202] , SLS [21,23,93] et PolyJet [25,90,146,156,165,203]) seem to provide similar results. For instance, Wingrove et al. [25](SLA) and Moraga-Espinosa et al. [88] (PolyJet) find, for liquid sprays having similar angles, similar deposition profiles (around 50% in the anterior region and 50%

in the turbinate region for a 37° plume angle). The accuracy and surface finish of all these techniques being comparable, it is not surprising to find out that the deposition patterns are very close between these casts.

Some teams use nasal casts that are not produced by 3D printing but by milling thin acrylic sheet to build, layer by layer, a complete nasal replica [154,159,204]. However, this technique is used by older studies when 3D printing was not as widespread as today. While being very precise, milling requires expensive equipment and skilled staff, which are not needed for 3D printing [206]. For these reasons, 3D printing replaced milling in cast production.

Finally, an educational cast, made by Koken, is also used for nasal spray deposition studies (Figure 12f) [89,162,205]. However, a research team reported that the shape of this replica differs from the median adult [207]. In particular, the nasal valve shape is drastically different and is believed to have a vast impact on the deposition pattern. Therefore, results obtained using this replica model should be considered with caution.

○ Use of synthetic mucus

All the previous steps, from the cast design to the choice of suitable 3D-printing technique, will lead to a cast geometry that reproduces the actual nasal cavities with the desired level of precision. However, 3D printing can only replicate the geometry and not the mucus surface and its particular adhesion properties. Consequently, the addition of synthetic mucus is often suitable. To this end, numerous solutions exist.

The interaction between a spray particle and the walls is reported to be drastically different if those are wet or dry [22,156], especially for powders that will bounce on dry walls [156]. *Sawant et al.* studied the administration of the same sprays in the same conditions, with and without mucus. They observed that the mean deposition in the cast increased from 32% to 38%, with the rest of the formulation dripping out. This study tends to prove the utility of such solutions [90].

The first category of artificial mucus mainly aims to provide a wet surface. Therefore, water [31] is a potential candidate to coat the cast. Mixtures such as ethanol and glycerol (75:25) [157] or propylene glycol and isopropyl alcohol (1:1 w/w) [156] also have been used to get higher viscosity. Arrhenius' formula [208] allows estimating their respective viscosities to around 5 and 8 mPa.s, which is still far from human mucus with a viscosity of about 12 Pa.s. Moreover, the mucus is a non-Newtonian fluid: the water alone cannot reproduce its complex rheological behaviour [209,210]. That is why more complex imitations have been developed [209,211]. They are aqueous solutions of galactomannan gum and scleroglucan. Their

viscosity may be modulated by changing the amount of scleroglucan (0.5% to 2% wt). This polymer combination allowed producing artificial mucus that has the main rheological characteristics of physiological mucus [211–213]. Up to now, this type of mucus has not been used in nasal casts yet.

The second category of artificial mucus uses glycerol [23] or ethanol [65] solutions with surfactants. They dry in the cast to create an adhesive surface without adding a liquid layer. Finally, the third category of artificial mucus are solutions of mucins [22]. Mucins are the main glycoproteins present in natural mucus. Their main advantage is to reproduce their interactions with the pharmaceutical formulation [210]. This type of mucus should be preferred if the formulation contains mucoadhesive components. Still, they do not have actual mucus viscosity. Consequently, they are not a perfect reproduction of this fluid [214]. Up to now, no study has compared the same drug administration with different mucus.

Another aspect to consider when choosing a mucus simulant is the affinity between the polymer and the mucus solution. Many polymers used to produce nasal casts are hydrophilic (Nylon:59.6°) [215] but their contact angles with water can be close to 90° (PLA: 80.8°, ABS: 84.7°) [215] and some are even hydrophobic (PP: 91.5°) [215]. Therefore, testing the spreading of the mucus on the surface is advised before deposition tests. Finally, as for the 3D-printing material, the mucus should not interfere with the analysis of the deposition. So, the artificial mucus should not contain molecules hiding the API signature in spectroscopy or chromatography.

Let us also mention that optical measurement using gel-like substances [26,89,146,162] see section 4.1) also leads to more adhesion on the cast while this is not their primary goal.

• Conclusion and challenges

This review highlighted the importance of pre-formulation in the development of new nose-to-brain drugs. In vivo tests proved that a good optimization beforehand leads to better bioavailability. Indeed, cautious pre-formulation can increase the residence time, decrease the mucociliary clearance and strengthen the permeation through the mucosa. For testing the obtained formulations more realistically than in vivo tests on mice, 3D-printed nasal casts represent a great interest.

Moreover, they can be adapted for each patient. So, it allows health professionals to create personalised administration protocols, maximising the amount of drug reaching the brain. Better nasal replicas would also lead to a better understanding of the key parameters to further

improve drug deposition on interest sites. This could lead to better design of instillation devices or even new concepts of administration. Better pieces of equipment could also provide clues for tailor-made formulations and for adjusting the existing strategies. However, their design should incorporate the study objectives to ensure an in vitro – in vivo correlation. To date, only a few teams studied in vitro – in vivo correlations. While some results are encouraging [25], others show that imprecision in cast conception can lead to no correlation [93].

In vivo is where most of the work is still needed. First, the properties of the formulation have been extensively tested on mice but not on humans. Therefore, clinical trials should be done to ensure that they are also valuable for patients. Second, 3D-printed casts should be compared to in vivo test to validate the test process. This way would ensure that the protocol developed in the lab also works in real-life conditions. This path is ambitious but it paves the way to new therapies targeting the central nervous system.

References

[1] V. Pandey, A. Gadeval, S. Asati, P. Jain, N. Jain, R.K. Roy, M. Tekade, V. Soni, R.K. Tekade, Formulation strategies for nose-to-brain delivery of therapeutic molecules, Elsevier Inc., 2019. https://doi.org/10.1016/B978-0-12-814487-9.00007-7.

[2] N.R. Hussein, H.K. Omer, A.M.A. Elhissi, W. Ahmed, Advances in nasal drug delivery systems, Elsevier Inc., 2020. https://doi.org/10.1016/b978-0-12-819712-7.00015-2.

[3] S. Moinuddin, S. Hasan Razvi, M. Fazil, M. Mustaneer Akmal, C. Syed Moinuddin, M. Shanawaz Uddin, S. Shahidulla, Nasal drug delivery system: A innovative approach, ~ 169 ~ Pharma Innov. J. 8 (2019) 169–177. www.thepharmajournal.com.

[4] F. Sabir, R. Ismail, I. Csoka, Nose-to-brain delivery of antiglioblastoma drugs embedded into lipid nanocarrier systems: status quo and outlook, Drug Discov. Today. 25 (2020) 185–194. https://doi.org/10.1016/j.drudis.2019.10.005.

[5] P.G. Upadhaya, S. Pulakkat, V.B. Patravale, Nose-to-brain delivery: exploring newer domains for glioblastoma multiforme management, Drug Deliv. Transl. Res. 10 (2020) 1044–1056. https://doi.org/10.1007/s13346-020-00747-y.

[6] A.D. Kulkarni, Y.H. Vanjari, K.H. Sancheti, V.S. Belgamwar, S.J. Surana, C. V. Pardeshi, Nanotechnology-mediated nose to brain drug delivery for Parkinson's disease: A mini review, J. Drug Target. 23 (2015) 775–788. https://doi.org/10.3109/1061186X.2015.1020809.

[7] M. Agrawal, S. Saraf, S. Saraf, S.G. Antimisiaris, M.B. Chougule, S.A. Shoyele, A. Alexander, Nose-to-brain drug delivery: An update on clinical challenges and progress towards approval of anti-Alzheimer drugs, J. Control. Release. 281 (2018) 139–177. https://doi.org/10.1016/j.jconrel.2018.05.011.

[8] A. Alexander, S. Saraf, Nose-to-brain drug delivery approach: A key to easily accessing the brain for the treatment of Alzheimer's disease, Neural Regen. Res. 13 (2018) 2102–2104. https://doi.org/10.4103/1673-5374.241458.

[9] B. Forbes, R. Bommer, J. Goole, M. Hellfritzsch, W. De Kruijf, P. Lambert, G.

Caivano, A. Regard, F. Schiaretti, M. Trenkel, L. Vecellio, G. Williams, F. Sonvico, R. Scherließ, A consensus research agenda for optimising nasal drug delivery, Expert Opin. Drug Deliv. 17 (2020) 127–132. https://doi.org/10.1080/17425247.2020.1714589.

[10] S.B. Yarragudi, H. Kumar, R. Jain, M. Tawhai, S. Rizwan, Olfactory Targeting of Microparticles through Inhalation and Bi-directional Airflow: Effect of Particle Size and Nasal Anatomy, J. Aerosol Med. Pulm. Drug Deliv. 33 (2020) 258–270. https://doi.org/10.1089/jamp.2019.1549.

[11] J.D. Schroeter, E.W. Tewksbury, B.A. Wong, J.S. Kimbell, Experimental Measurements and Computational Predictions of Regional Particle Deposition in a Sectional Nasal Model, J. Aerosol Med. Pulm. Drug Deliv. 28 (2015) 20–29. https://doi.org/10.1089/jamp.2013.1084.

[12] N.J. Johnson, L.R. Hanson, W.H. Frey, Trigeminal Pathways Deliver a Low Molecular Weight Drug from the Nose to the Brain and Orofacial Structures, Mol. Pharm. 7 (2010) 884–893. https://doi.org/10.1021/mp100029t.

[13] L. Illum, Transport of drugs from the nasal cavity to the central nervous system, Eur. J. Pharm. Sci. 11 (2000) 1–18. https://doi.org/10.1016/S0928-0987(00)00087-7.

[14] P.P. Martins, H.D.C.C. Smyth, Z. Cui, Strategies to facilitate or block nose-to-brain drug delivery, Int. J. Pharm. 570 (2019) 118635. https://doi.org/10.1016/j.ijpharm.2019.118635.

[15] M. Ghadiri, P.M. Young, D. Traini, Strategies to enhance drug absorption via nasal and pulmonary routes, Pharmaceutics. 11 (2019) 1–20. https://doi.org/10.3390/pharmaceutics11030113.

[16] H. Kumar, G. Mishra, A.K. Sharma, A. Gothwal, P. Kesharwani, U. Gupta, Intranasal Drug Delivery: A Non-Invasive Approach for the Better Delivery of Neurotherapeutics, Pharm. Nanotechnol. 5 (2017). https://doi.org/10.2174/2211738505666170515113936.

[17] Z.E. Jassim, E.J. Al-akkam, A review on strategies for improving nasal drug delivery systems, Drug Invent. Today. 10 (2018) 1–9.

[18] A. Alexander, M. Agrawal, A. Uddin, S. Siddique, A.M. Shehata, M.A. Shaker, S. Ata Ur Rahman, M.I.M. Abdul, M.A. Shaker, Recent expansions of novel strategies towards the drug targeting into the brain, Int. J. Nanomedicine. Volume 14 (2019) 5895–5909. https://doi.org/10.2147/IJN.S210876.

[19] P. Le Corre, Administration intranasale des médicaments pour une action systémique, La Lett. Du Pharmacol. 15 (2001) 167–174. https://www.edimark.fr/lettre-pharmacologue/administration-intranasale-medicaments-action-systemique.

[20] X.B. Chen, H.P. Lee, V.F. Hin Chong, D.Y. Wang, Assessment of septal deviation effects on nasal air flow: A computational fluid dynamics model: Nasal Air Flow with Septal Deviation, Laryngoscope. 119 (2009) 1730–1736. https://doi.org/10.1002/lary.20585.

[21] R. Hughes, J. Watterson, C. Dickens, D. Ward, A. Banaszek, Development of a nasal cast model to test medicinal nasal devices, Proc. Inst. Mech. Eng. Part H J. Eng. Med. 222 (2008) 1013–1022. https://doi.org/10.1243/09544119JEIM423.

[22] N. Sawant, M.D. Donovan, In Vitro Assessment of Spray Deposition Patterns in a Pediatric (12 Year-Old) Nasal Cavity Model, Pharm. Res. 35 (2018). https://doi.org/10.1007/s11095-018-2385-6.

[23] S.A. Shah, C.J. Dickens, D.J. Ward, A.A. Banaszek, C. George, W. Horodnik, Design of Experiments to Optimize an In Vitro Cast to Predict Human Nasal Drug Deposition, J. Aerosol Med. Pulm. Drug Deliv. 27 (2014) 21–29. https://doi.org/10.1089/jamp.2012.1011.

[24] Z.N. Warnken, H.D.C.C. Smyth, D.A. Davis, S. Weitman, J.G. Kuhn, R.O. Williams, Personalized Medicine in Nasal Delivery: The Use of Patient-Specific Administration Parameters To Improve Nasal Drug Targeting Using 3D-Printed Nasal Replica Casts, Mol. Pharm. 15 (2018) 1392–1402. https://doi.org/10.1021/acs.molpharmaceut.7b00702.

[25] J. Wingrove, M. Swedrowska, R. Scherließ, M. Parry, M. Ramjeeawon, D. Taylor, G. Gauthier, L. Brown, S. Amiel, F. Zelaya, B. Forbes, Characterisation of nasal devices for delivery of insulin to the brain and evaluation in humans using functional magnetic resonance imaging, J. Control. Release. 302 (2019) 140–147. https://doi.org/10.1016/j.jconrel.2019.03.032.

[26] J. Xi, J.E. Yuan, Y. Zhang, D. Nevorski, Z. Wang, Y. Zhou, Visualization and Quantification of Nasal and Olfactory Deposition in a Sectional Adult Nasal Airway Cast, Pharm. Res. 33 (2016) 1527–1541. https://doi.org/10.1007/s11095-016-1896-2.

[27] S. Le Guellec, S. Ehrmann, L. Vecellio, In vitro – in vivo correlation of intranasal drug deposition, Adv. Drug Deliv. Rev. (2020). https://doi.org/10.1016/j.addr.2020.09.002.

[28] G. Verma, M.K. Mishra, Pharmaceutical Preformulation Studies in Formulation and Development of New Dosage Form: A Review, Int. J. Pharma Res. Rev. 5 (2016) 12–20.

[29] K. Vilegave, G. Vidyasagar, P. Chandankar, Preformulation Studies of Pharmaceutical New Drug Molecule & Products: An Overview, Am. J. Pharm. Heal. Res. 1 (2013) 1–20. www.ajphr.com.

[30] R. Gopinath, R. a S. Naidu, Pharmaceutical Preformulation Studies – Current Review, Int. J. Pharm. Biol. Arch. 2 (2011) 1391–1400.

[31] L. Salade, N. Wauthoz, M. Vermeersch, K. Amighi, J. Goole, Chitosan-coated liposome dry-powder formulations loaded with ghrelin for nose-to-brain delivery, Eur. J. Pharm. Biopharm. 129 (2018) 257–266. https://doi.org/10.1016/j.ejpb.2018.06.011.

[32] V. V Ranade, Biotechnology: Pharmaceutical Aspects, 2010. https://doi.org/10.1097/mjt.0b013e31817c947a.

[33] V. Borhade, S. Pathak, S. Sharma, V. Patravale, Clotrimazole nanoemulsion for malaria chemotherapy. Part I: Preformulation studies, formulation design and physicochemical evaluation, Int. J. Pharm. 431 (2012) 138–148. https://doi.org/10.1016/j.ijpharm.2011.12.040.

[34] K. Patel, S. Padhye, M. Nagarsenker, Duloxetine HCl lipid nanoparticles: Preparation, characterization, and dosage form design, AAPS PharmSciTech. 13 (2012) 125–133. https://doi.org/10.1208/s12249-011-9727-6.

[35] H. Shete, V. Patravale, Long chain lipid based tamoxifen NLC. Part I: Preformulation studies, formulation development and physicochemical characterization, Int. J. Pharm. 454 (2013) 573–583. https://doi.org/10.1016/j.ijpharm.2013.03.034.

[36] L. Illum, Nasal drug delivery: New developments and strategies, Drug Discov. Today. 7 (2002) 1184–1189. https://doi.org/10.1016/S1359-6446(02)02529-1.

[37] M.S.A. Tan, H.S. Parekh, P. Pandey, D.J. Siskind, J.R. Falconer, Nose-to-brain delivery of antipsychotics using nanotechnology: a review, Expert Opin. Drug Deliv. 17 (2020) 839–853. https://doi.org/10.1080/17425247.2020.1762563.

[38] S.K.S. Kushwaha, R.K. Keshari, A.K. Rai, Advances in nasal trans-mucosal drug delivery, J. Appl. Pharm. Sci. 1 (2011) 21–28.

[39] P. Arora, S. Sharma, S. Garg, Permeability issues in nasal drug delivery, Drug Discov. Today. 7 (2002) 967–975. https://doi.org/10.1016/S1359-6446(02)02452-2.

[40] X. Liu, B. Testa, A. Fahr, Lipophilicity and its relationship with passive drug permeation, Pharm. Res. 28 (2011) 962–977. https://doi.org/10.1007/s11095-010-0303-7.

[41] S. Bahadur, K. Pathak, Physicochemical and physiological considerations for efficient nose-to-brain targeting, Expert Opin. Drug Deliv. 9 (2012) 19–31. https://doi.org/10.1517/17425247.2012.636801.
[42] A. Giuliani, A.G. Balducci, E. Zironi, G. Colombo, F. Bortolotti, L. Lorenzini, V. Galligioni, G. Pagliuca, A. Scagliarini, L. Calzà, F. Sonvico, In vivo nose-to-brain delivery of the hydrophilic antiviral ribavirin by microparticle agglomerates, Drug Deliv. 25 (2018) 376–387. https://doi.org/10.1080/10717544.2018.1428242.
[43] S. Md, G. Mustafa, S. Baboota, J. Ali, Nanoneurotherapeutics approach intended for direct nose to brain delivery, Drug Dev. Ind. Pharm. 41 (2015) 1922–1934. https://doi.org/10.3109/03639045.2015.1052081.
[44] L.H. Salem, G.S. El-Feky, R.H. Fahmy, O.N. El Gazayerly, A. Abdelbary, Coated Lipidic Nanoparticles as a New Strategy for Enhancing Nose-to-Brain Delivery of a Hydrophilic Drug Molecule, J. Pharm. Sci. 109 (2020) 2237–2251. https://doi.org/10.1016/j.xphs.2020.04.007.
[45] G. Butcher, J. Comer, A. Avdeef, pKa-critical interpretations of solubility-pH Profiles: PG-300995 and NSC-639829 case studies, ADMET DMPK. 3 (2015) 131–140. https://doi.org/10.5599/admet.3.2.182.
[46] T. Lin, E. Liu, H. He, M.C. Shin, C. Moon, V.C. Yang, Y. Huang, Nose-to-brain delivery of macromolecules mediated by cell-penetrating peptides, Acta Pharm. Sin. B. 6 (2016) 352–358. https://doi.org/10.1016/j.apsb.2016.04.001.
[47] L. Yan, H. Wang, Y. Jiang, J. Liu, Z. Wang, Y. Yang, S. Huang, Y. Huang, Cell-penetrating peptide-modified PLGA nanoparticles for enhanced nose-to-brain macromolecular delivery, Macromol. Res. 21 (2013) 435–441. https://doi.org/10.1007/s13233-013-1029-2.
[48] C. McMartin, L.E.F. Hutchinson, R. Hyde, G.E. Peters, Analysis of Structural Requirements for the Absorption of Drugs and Macromolecules from the Nasal Cavity, J. Pharm. Sci. 76 (1987) 535–540. https://doi.org/10.1002/jps.2600760709.
[49] A. Rygg, M. Hindle, P.W. Longest, Linking Suspension Nasal Spray Drug Deposition Patterns to Pharmacokinetic Profiles: A Proof-of-Concept Study Using Computational Fluid Dynamics, J. Pharm. Sci. 105 (2016) 1995–2004. https://doi.org/10.1016/j.xphs.2016.03.033.
[50] H.E. Huber, W.H. Streng, H.G.H. Tan, Osmolality of parenteral solutions, J. Pharm. Sci. 68 (1979) 1028–1032. https://doi.org/10.1002/jps.2600680829.
[51] Ç.Y.A. et C.J. M., Fluid mechanics: fundamentals and applications, 3e edition, 2014, New York, n.d.
[52] N. Hussein, H. Omer, A. Ismael, M. Albed Alhnan, A. Elhissi, W. Ahmed, Spray-dried alginate microparticles for potential intranasal delivery of ropinirole hydrochloride: development, characterization and histopathological evaluation, Pharm. Dev. Technol. 25 (2020) 290–299. https://doi.org/10.1080/10837450.2019.1567762.
[53] J.B. Prajapati, G.C. Patel, Nose to brain delivery of Rotigotine loaded solid lipid nanoparticles: Quality by Design based optimization and characterization, J. Drug Deliv. Sci. Technol. (2021) 102377. https://doi.org/10.1016/j.jddst.2021.102377.
[54] S. Cometa, M.A. Bonifacio, G. Trapani, S. Di Gioia, L. Dazzi, E. De Giglio, A. Trapani, In vitro investigations on dopamine loaded Solid Lipid Nanoparticles, J. Pharm. Biomed. Anal. 185 (2020). https://doi.org/10.1016/j.jpba.2020.113257.
[55] A. V. Belgamwar, S.A. Khan, P.G. Yeole, Intranasal dolutegravir sodium loaded nanoparticles of hydroxypropyl-beta-cyclodextrin for brain delivery in Neuro-AIDS, J. Drug Deliv. Sci. Technol. 52 (2019) 1008–1020. https://doi.org/10.1016/j.jddst.2019.06.014.
[56] A.K. Singh, A. Gothwal, S. Rani, M. Rana, A.K. Sharma, A.K. Yadav, U. Gupta,

Dendrimer donepezil conjugates for improved brain delivery and better in vivo pharmacokinetics, ACS Omega. 4 (2019) 4519–4528. https://doi.org/10.1021/acsomega.8b03445.
[57] S. Rajarajan, B.P. Rao, S. Selvamuthukumar, Design and Development of Chitosan Beta-cyclodextrin based Nasal Mucoadhesive Microspheres of Clarithromycin, Int. J. Pharm. Investig. 10 (2020) 279–285. https://doi.org/10.5530/ijpi.2020.3.51.
[58] A.P. Matarazzo, L.M.S. Elisei, F.C. Carvalho, R. Bonfílio, A.L.M. Ruela, G. Galdino, G.R. Pereira, Mucoadhesive nanostructured lipid carriers as a cannabidiol nasal delivery system for the treatment of neuropathic pain, Eur. J. Pharm. Sci. 159 (2021). https://doi.org/10.1016/j.ejps.2020.105698.
[59] M. Qureshi, M. Aqil, S.S. Imam, A. Ahad, Y. Sultana, Formulation and Evaluation of Neuroactive Drug Loaded Chitosan Nanoparticle for Nose to Brain Delivery: In-vitro Characterization and In-vivo Behavior Study, Curr. Drug Deliv. 16 (2018) 123–135. https://doi.org/10.2174/1567201815666181011121750.
[60] I. Ledeti, S. Bolintineanu, G. Vlase, D. Circioban, A. Ledeti, T. Vlase, L.M. Suta, A. Caunii, M. Murariu, Compatibility study between antiparkinsonian drug Levodopa and excipients by FTIR spectroscopy, X-ray diffraction and thermal analysis, J. Therm. Anal. Calorim. 130 (2017) 433–441. https://doi.org/10.1007/s10973-017-6393-2.
[61] M. Masjedi, A. Azadi, R. Heidari, S. Mohammadi-Samani, Nose-to-brain delivery of sumatriptan-loaded nanostructured lipid carriers: preparation, optimization, characterization and pharmacokinetic evaluation, J. Pharm. Pharmacol. 72 (2020) 1341–1351. https://doi.org/10.1111/jphp.13316.
[62] S. Arisoy, O. Sayiner, T. Comoglu, D. Onal, O. Atalay, B. Pehlivanoglu, In vitro and in vivo evaluation of levodopa-loaded nanoparticles for nose to brain delivery, Pharm. Dev. Technol. 25 (2020) 735–747. https://doi.org/10.1080/10837450.2020.1740257.
[63] D.M. Vasa, I.S. Buckner, J.E. Cavanaugh, P.L.D. Wildfong, Improved Flux of Levodopa via Direct Deposition of Solid Microparticles on Nasal Tissue, AAPS PharmSciTech. 18 (2017) 904–912. https://doi.org/10.1208/s12249-016-0581-4.
[64] S.H. Wang, S.M. Kirwan, S.N. Abraham, H.F. Staats, A.J. Hickey, Stable dry powder formulation for nasal delivery of anthrax vaccine, J. Pharm. Sci. 101 (2012) 31–47. https://doi.org/10.1002/jps.22742.
[65] S.G. Thakkar, Z.N. Warnken, R.F. Alzhrani, S.A. Valdes, A.M. Aldayel, H. Xu, R.O. Williams, Z. Cui, Intranasal immunization with aluminum salt-adjuvanted dry powder vaccine, J. Control. Release. 292 (2018) 111–118. https://doi.org/10.1016/j.jconrel.2018.10.020.
[66] K.B. Preston, T.W. Randolph, Stability of lyophilized and spray dried vaccine formulations, Adv. Drug Deliv. Rev. (2021). https://doi.org/10.1016/j.addr.2021.01.016.
[67] E. García Esteban, M.J. Cózar-Bernal, A.M. Rabasco Álvarez, M.L. González-Rodríguez, A comparative study of stabilising effect and antioxidant activity of different antioxidants on levodopa-loaded liposomes, J. Microencapsul. 35 (2018) 357–371. https://doi.org/10.1080/02652048.2018.1487473.
[68] C. von Halling Laier, B. Gibson, M. van de Weert, B.J. Boyd, T. Rades, A. Boisen, S. Hook, L.H. Nielsen, Spray dried cubosomes with ovalbumin and Quil-A as a nanoparticulate dry powder vaccine formulation, Int. J. Pharm. 550 (2018) 35–44. https://doi.org/10.1016/j.ijpharm.2018.08.036.
[69] S. Patel, S. Chavhan, H. Soni, A.K. Babbar, R. Mathur, A.K. Mishra, K. Sawant, Brain targeting of risperidone-loaded solid lipid nanoparticles by intranasal route, J. Drug Target. 19 (2011) 468–474. https://doi.org/10.3109/1061186X.2010.523787.
[70] Z. Hussain, S. Sahudin, Preparation, characterisation and colloidal stability of chitosan-

tripolyphosphate nanoparticles: Optimisation of formulation and process parameters, Int. J. Pharm. Pharm. Sci. 8 (2016) 297–308.
[71] P. Keshari, Y. Sonar, H. Mahajan, Curcumin loaded TPGS micelles for nose to brain drug delivery: in vitro and in vivo studies, Mater. Technol. 34 (2019) 423–432. https://doi.org/10.1080/10667857.2019.1575535.
[72] S.K. Bhattamisra, A.T. Shak, L.W. Xi, N.H. Safian, H. Choudhury, W.M. Lim, N. Shahzad, N.A. Alhakamy, M.K. Anwer, A.K. Radhakrishnan, S. Md, Nose to brain delivery of rotigotine loaded chitosan nanoparticles in human SH-SY5Y neuroblastoma cells and animal model of Parkinson's disease, Int. J. Pharm. 579 (2020). https://doi.org/10.1016/j.ijpharm.2020.119148.
[73] M.R.S. Sara Assadpour, J. Akhtari, Chitosan coating of anionic liposomes containing sumatriptan succinate : a candidate for nasal administration, Nanomed. J. 8(2). 8 (2021). https://doi.org/10.22038/nmj.2021.08.002.
[74] R.P. Patil, D.D. Pawara, C.S. Gudewar, A.R. Tekade, Nanostructured cubosomes in an in situ nasal gel system: an alternative approach for the controlled delivery of donepezil HCl to brain, J. Liposome Res. 29 (2019) 264–273. https://doi.org/10.1080/08982104.2018.1552703.
[75] C.P. Pujara, Z. Shao, M.R. Duncan, A.K. Mitra, Effects of formulation variables on nasal epithelial cell integrity: Biochemical evaluations, Int. J. Pharm. 114 (1995) 197–203. https://doi.org/10.1016/0378-5173(94)00238-Z.
[76] R. Dua, H. Zia, T. Needham, The influence of tonicity and viscosity on the intranasal absorption of salmon calcitonin in rabbits, Int. J. Pharm. 147 (1997) 233–242. https://doi.org/10.1016/S0378-5173(96)04817-X.
[77] J.C. Olivier, M. Djilani, S. Fahmy, W. Couet, In situ nasal absorption of midazolam in rats, Int. J. Pharm. 213 (2001) 187–192. https://doi.org/10.1016/S0378-5173(00)00668-2.
[78] J.J. Homer, A.C. Dowley, L. Condon, P. El-Jassar, S. Sood, The effect of hypertonicity on nasal mucociliary clearance, Clin. Otolaryngol. Allied Sci. 25 (2000) 558–560. https://doi.org/10.1046/j.1365-2273.2000.00420.x.
[79] FDA, Inactive Ingredients Database Download, (2021). https://www.fda.gov/drugs/drug-approvals-and-databases/inactive-ingredients-database-download (accessed February 16, 2021).
[80] F. Wang, Z. Yang, M. Liu, Y. Tao, Z. Li, Z. Wu, S. Gui, Facile nose-to-brain delivery of rotigotine-loaded polymer micelles thermosensitive hydrogels: In vitro characterization and in vivo behavior study, Int. J. Pharm. 577 (2020) 1–9. https://doi.org/10.1016/j.ijpharm.2020.119046.
[81] A.D. Kulkarni, D.B. Bari, S.J. Surana, C. V. Pardeshi, In vitro, ex vivo and in vivo performance of chitosan-based spray-dried nasal mucoadhesive microspheres of diltiazem hydrochloride, J. Drug Deliv. Sci. Technol. 31 (2016) 108–117. https://doi.org/10.1016/j.jddst.2015.12.004.
[82] Y.S. Kim, D.K. Sung, H. Kim, W.H. Kong, Y.E. Kim, S.K. Hahn, Nose-to-brain delivery of hyaluronate – FG loop peptide conjugate for non-invasive hypoxic-ischemic encephalopathy therapy, J. Control. Release. 307 (2019) 76–89. https://doi.org/10.1016/j.jconrel.2019.06.021.
[83] D.A.E. Mostafa, M.K.A. Khalifa, S.S. Gad, Zolmitriptan brain targeting via intranasal route using solid lipid nanoparticles for migraine therapy: Formulation, characterization, in-vitro and in-vivo assessment, Int. J. Appl. Pharm. 12 (2020) 86–93. https://doi.org/10.22159/ijap.2020v12i2.36812.
[84] E.Y. Lin, Y.S. Chen, Y.S. Li, S.R. Chen, C.H. Lee, M.H. Huang, H.M. Chuang, H.J. Harn, H.H. Yang, S.Z. Lin, D.F. Tai, T.W. Chiou, Liposome consolidated with

cyclodextrin provides prolonged drug retention resulting in increased drug bioavailability in brain, Int. J. Mol. Sci. 21 (2020) 1–17. https://doi.org/10.3390/ijms21124408.
[85] S.T. Charlton, S.S. Davis, L. Illum, Evaluation of bioadhesive polymers as delivery systems for nose to brain delivery : In vitro characterisation studies, 118 (2007) 225–234. https://doi.org/10.1016/j.jconrel.2006.12.014.
[86] T. Furubayashi, D. Inoue, A. Kamaguchi, Y. Higashi, T. Sakane, Influence of Formulation Viscosity on Drug Absorption Following Nasal Application in Rats, Drug Metab. Pharmacokinet. 22 (2007) 206–211. https://doi.org/10.2133/dmpk.22.206.
[87] P.C. Pires, L.T. Santos, M. Rodrigues, G. Alves, A.O. Santos, Intranasal fosphenytoin: The promise of phosphate esters in nose-to-brain delivery of poorly soluble drugs, Int. J. Pharm. 592 (2021). https://doi.org/10.1016/j.ijpharm.2020.120040.
[88] D. Moraga-Espinoza, Z. Warnken, A. Moore, R.O. Williams, H.D.C.C. Smyth, A modified USP induction port to characterize nasal spray plume geometry and predict turbinate deposition under flow, Int. J. Pharm. 548 (2018) 305–313. https://doi.org/10.1016/j.ijpharm.2018.06.058.
[89] Y. Pu, A.P. Goodey, X. Fang, K. Jacob, A Comparison of the Deposition Patterns of Different Nasal Spray Formulations Using a Nasal Cast, Aerosol Sci. Technol. 48 (2014) 930–938. https://doi.org/10.1080/02786826.2014.931566.
[90] N. Sawant, M.D. Donovan, In Vitro Assessment of Spray Deposition Patterns in a Pediatric (12 Year-Old) Nasal Cavity Model, Pharm. Res. 35 (2018). https://doi.org/10.1007/s11095-018-2385-6.
[91] H. Shi, C. Kleinstreuer, Z. Zhang, Modeling of inertial particle transport and deposition in human nasal cavities with wall roughness, J. Aerosol Sci. 38 (2007) 398–419. https://doi.org/10.1016/j.jaerosci.2007.02.002.
[92] H. Calmet, K. Inthavong, B. Eguzkitza, O. Lehmkuhl, G. Houzeaux, M. Vázquez, Nasal sprayed particle deposition in a human nasal cavity under different inhalation conditions, PLoS One. 14 (2019) e0221330–e0221330. https://doi.org/10.1371/journal.pone.0221330.
[93] S.A. Shah, R.L. Berger, J. McDermott, P. Gupta, D. Monteith, A. Connor, W. Lin, Regional deposition of mometasone furoate nasal spray suspension in humans, Allergy Asthma Proc. 36 (2015) 48–57. https://doi.org/10.2500/aap.2015.36.3817.
[94] M. Kiaee, H. Wachtel, M.L. Noga, A.R. Martin, W.H. Finlay, Regional deposition of nasal sprays in adults: {A} wide ranging computational study, Int. j. Numer. Method. Biomed. Eng. 34 (2018) e2968–e2968. https://doi.org/10.1002/cnm.2968.
[95] O. Samia, R. Hanan, E.T. Kamal, Carbamazepine Mucoadhesive Nanoemulgel (MNEG) as brain targeting delivery system via the olfactory mucosa, Drug Deliv. 19 (2012) 58–67. https://doi.org/10.3109/10717544.2011.644349.
[96] M.M. Migliore, T.K. Vyas, R.B. Campbell, M.M. Amiji, B.L. Waszczak, Brain delivery of proteins by the intranasal route of administration: {A} comparison of cationic liposomes versus aqueous solution formulations, J. Pharm. Sci. 99 (2010) 1745–1761. https://doi.org/10.1002/jps.21939.
[97] H. Takeuchi, K. Imamura, B. Ji, K. Tsukita, T. Enami, K. Takao, T. Miyakawa, M. Hasegawa, N. Sahara, N. Iwata, M. Inoue, H. Hara, T. Tabira, M. Ono, J.Q. Trojanowski, V.M.-Y. Lee, R. Takahashi, T. Suhara, M. Higuchi, H. Inoue, Nasal vaccine delivery attenuates brain pathology and cognitive impairment in tauopathy model mice, Npj Vaccines. 5 (2020) 28. https://doi.org/10.1038/s41541-020-0172-y.
[98] G. Pilcer, K. Amighi, Formulation strategy and use of excipients in pulmonary drug delivery, Int. J. Pharm. 392 (2010) 1–19. https://doi.org/10.1016/j.ijpharm.2010.03.017.

[99] H.W. C., Aerosol technology: properties, behavior, and measurement of airborne particles, 2e edition, 1999, New York, n.d.
[100] L. Tiozzo Fasiolo, M.D. Manniello, F. Bortolotti, F. Buttini, A. Rossi, F. Sonvico, P. Colombo, G. Valsami, G. Colombo, P. Russo, Anti-inflammatory flurbiprofen nasal powders for nose-to-brain delivery in Alzheimer's disease, J. Drug Target. 27 (2019) 984–994. https://doi.org/10.1080/1061186X.2019.1574300.
[101] A. Di, S. Zhang, X. Liu, Z. Tong, S. Sun, Z. Tang, X.D. Chen, W.D. Wu, Microfluidic spray dried and spray freeze dried uniform microparticles potentially for intranasal drug delivery and controlled release, Powder Technol. 379 (2021) 144–153. https://doi.org/10.1016/j.powtec.2020.10.061.
[102] M. Keyhan shokouh, H. Faghihi, M. Darabi, M. Mirmoeini, A. Vatanara, Formulation and evaluation of inhalable microparticles of Rizatriptan Benzoate processed by spray freeze-drying, J. Drug Deliv. Sci. Technol. 62 (2021). https://doi.org/10.1016/j.jddst.2021.102356.
[103] A. Goldstein, Y. Soroka, M. Frušić-Zlotkin, I. Popov, R. Kohen, High resolution SEM imaging of gold nanoparticles in cells and tissues, J. Microsc. 256 (2014) 237–247. https://doi.org/10.1111/jmi.12179.
[104] S.C. Leong, X.B. Chen, H.P. Lee, D.Y. Wang, A review of the implications of computational fluid dynamic studies on nasal airflow and physiology, Rhinol. J. 48 (2010). https://doi.org/10.4193/Rhin09.133.
[105] A. Jüptner, R. Scherließ, Spray dried formulations for inhalation—meaningful characterisation of powder properties, Pharmaceutics. 12 (2020). https://doi.org/10.3390/pharmaceutics12010014.
[106] E. Marttin, N.G.M. Schipper, J. Coos Verhoef, F.W.H.M. Merkus, Nasal mucociliary clearance as a factor in nasal drug delivery, Adv. Drug Deliv. Rev. 29 (1998) 13–38. https://doi.org/10.1016/S0169-409X(97)00059-8.
[107] L. Illum, Is nose-to-brain transport of drugs in man a reality?, J. Pharm. Pharmacol. 56 (2010) 3–17. https://doi.org/10.1211/0022357022539.
[108] S. Ladel, P. Schlossbauer, J. Flamm, H. Luksch, B. Mizaikoff, K. Schindowski, Improved in vitro model for intranasal mucosal drug delivery: Primary olfactory and respiratory epithelial cells compared with the permanent Nasal cell line RPMI 2650, Pharmaceutics. 11 (2019). https://doi.org/10.3390/pharmaceutics11080367.
[109] P.A. Escada, C. Lima, J.M. Da Silva, The human olfactory mucosa, Eur. Arch. Oto-Rhino-Laryngology. 266 (2009) 1675–1680. https://doi.org/10.1007/s00405-009-1073-x.
[110] G. Rassu, E. Soddu, M. Cossu, E. Gavini, P. Giunchedi, A. Dalpiaz, Particulate formulations based on chitosan for nose-to-brain delivery of drugs. A review, J. Drug Deliv. Sci. Technol. 32 (2016) 77–87. https://doi.org/10.1016/j.jddst.2015.05.002.
[111] E.R. de Oliveira Junior, T.L. Nascimento, M.A. Salomão, A.C.G. da Silva, M.C. Valadares, E.M. Lima, Increased Nose-to-Brain Delivery of Melatonin Mediated by Polycaprolactone Nanoparticles for the Treatment of Glioblastoma, Pharm. Res. 36 (2019). https://doi.org/10.1007/s11095-019-2662-z.
[112] J. Pandey, R. Shankar, M. Kumar, K. Shukla, B. Kumari, Development of Nasal Mucoadhesive Microspheres of Granisetron: A Potential Drug, Drug Res. (Stuttg). 70 (2020) 367–375. https://doi.org/10.1055/a-1193-4781.
[113] M. Kabiri, H. Bolourian, S. Dehghan, M. Tafaghodi, The dry powder formulation of mixed cross-linked dextran microspheres and tetanus toxoid-loaded trimethyl chitosan nanospheres as a potent adjuvant for nasal delivery system, Iran. J. Basic Med. Sci. 24 (2020) 116–122. https://doi.org/10.22038/ijbms.2020.49486.11313.
[114] U. Garg, S. Chauhan, U. Nagaich, N. Jain, Current Advances in Chitosan Nanoparticles

Based Drug Delivery and Targeting, Adv. Pharm. Bull. 9 (2019) 195–204. https://doi.org/10.15171/apb.2019.023.
[115] G. Rassu, L. Ferraro, B. Pavan, P. Giunchedi, E. Gavini, A. Dalpiaz, The role of combined penetration enhancers in nasal microspheres on in vivo drug bioavailability, Pharmaceutics. 10 (2018) 8–10. https://doi.org/10.3390/pharmaceutics10040206.
[116] R. Popescu, M.V. Ghica, C.E. Dinu-Pîrvu, V. Anuța, D. Lupuliasa, L. Popa, New opportunity to formulate intranasal vaccines and drug delivery systems based on chitosan, Int. J. Mol. Sci. 21 (2020) 1–23. https://doi.org/10.3390/ijms21145016.
[117] K. Manta, P. Papakyriakopoulou, M. Chountoulesi, D.A. Diamantis, D. Spaneas, V. Vakali, N. Naziris, M. V. Chatziathanasiadou, I. Andreadelis, K. Moschovou, I. Athanasiadou, P. Dallas, D.M. Rekkas, C. Demetzos, G. Colombo, S. Banella, U. Javornik, J. Plavec, T. Mavromoustakos, A.G. Tzakos, G. Valsami, Preparation and Biophysical Characterization of Quercetin Inclusion Complexes with β-Cyclodextrin Derivatives to be Formulated as Possible Nose-to-Brain Quercetin Delivery Systems, Mol. Pharm. 17 (2020) 4241–4255. https://doi.org/10.1021/acs.molpharmaceut.0c00672.
[118] P. Yang, Y. Li, W. Li, H. Zhang, J. Gao, J. Sun, X. Yin, A. Zheng, Preparation and evaluation of carfentanil nasal spray employing cyclodextrin inclusion technology, Drug Dev. Ind. Pharm. 44 (2018) 953–960. https://doi.org/10.1080/03639045.2018.1425426.
[119] M.A. Strege, S. Huang, D.S. Risley, Quantitative determination of beta-cyclodextrin in a powder insulin formulation for nasal delivery using hydrophilic interaction chromatography with evaporative light scattering detection, J. Liq. Chromatogr. Relat. Technol. 42 (2019) 74–78. https://doi.org/10.1080/10826076.2019.1571508.
[120] S.S. Davis, L. Illum, Absorption Enhancers for Nasal Drug Delivery, Clin. Pharmacokinet. 42 (2003) 1107–1128. https://doi.org/10.2165/00003088-200342130-00003.
[121] L. Illum, F. Jordan, A.L. Lewis, CriticalSorb^{TM}: A novel efficient nasal delivery system for human growth hormone based on Solutol HS15, J. Control. Release. 162 (2012) 194–200. https://doi.org/10.1016/j.jconrel.2012.06.014.
[122] L. Tiozzo Fasiolo, M.D. Manniello, E. Tratta, F. Buttini, A. Rossi, F. Sonvico, F. Bortolotti, P. Russo, G. Colombo, Opportunity and challenges of nasal powders: Drug formulation and delivery, Eur. J. Pharm. Sci. 113 (2018) 2–17. https://doi.org/10.1016/j.ejps.2017.09.027.
[123] N. Fransén, S. Bredenberg, E. Björk, Clinical study shows improved absorption of desmopressin with novel formulation, Pharm. Res. 26 (2009) 1618–1625. https://doi.org/10.1007/s11095-009-9871-9.
[124] G.J.M. Garcia, J.D. Schroeter, J.S. Kimbell, Olfactory deposition of inhaled nanoparticles in humans, Inhal. Toxicol. 27 (2015) 394–403. https://doi.org/10.3109/08958378.2015.1066904.
[125] H. Yusuf, V. Kett, Current prospects and future challenges for nasal vaccine delivery, Hum. Vaccines Immunother. 13 (2017) 34–45. https://doi.org/10.1080/21645515.2016.1239668.
[126] M. Agrawal, S. Saraf, S. Saraf, S.K. Dubey, A. Puri, U. Gupta, P. Kesharwani, V. Ravichandiran, P. Kumar, V.G.M. Naidu, U.S. Murty, Ajazuddin, A. Alexander, Stimuli-responsive In situ gelling system for nose-to-brain drug delivery, J. Control. Release. 327 (2020) 235–265. https://doi.org/10.1016/j.jconrel.2020.07.044.
[127] Q. Wang, Z. Zuo, C.K.C. Cheung, S.S.Y. Leung, B.A. Aderibigbe, Q. Wang, Z. Zuo, C.K.C. Cheung, S.S.Y. Leung, Updates on thermosensitive hydrogel for nasal, ocular and cutaneous delivery, Pharmaceutics. 559 (2019) 86–101.

https://doi.org/10.1016/j.ijpharm.2019.01.030.
[128] Q. Wang, Z. Zuo, C.K.C. Cheung, S.S.Y. Leung, Updates on thermosensitive hydrogel for nasal, ocular and cutaneous delivery, Int. J. Pharm. 559 (2019) 86–101. https://doi.org/10.1016/j.ijpharm.2019.01.030.
[129] H. Akel, R. Ismail, I. Csóka, M.S.A. Tan, H.S. Parekh, P. Pandey, D.J. Siskind, J.R. Falconer, T. Musumeci, A. Bonaccorso, G. Puglisi, H. Akel, R. Ismail, I. Csóka, M.R. Patel, R.B. Patel, K.K. Bhatt, B.G. Patel, R. V. Gaikwad, N. Delivery, N.A. Alhakamy, H.M. Aldawsari, H.Z. Asfour, Progress and perspectives of brain-targeting lipid-based nanosystems via the nasal route in Alzheimer's disease, Eur. J. Pharm. Biopharm. 148 (2020) 38–53. https://doi.org/10.1016/j.ejpb.2019.12.014.
[130] L. Battaglia, P.P. Panciani, E. Muntoni, M.T. Capucchio, E. Biasibetti, P. De Bonis, S. Mioletti, M. Fontanella, S. Swaminathan, Lipid nanoparticles for intranasal administration: application to nose-to-brain delivery, Expert Opin. Drug Deliv. 15 (2018) 369–378. https://doi.org/10.1080/17425247.2018.1429401.
[131] S. Cunha, C.P. Costa, J.A. Loureiro, J. Alves, A.F. Peixoto, B. Forbes, J.M.S. Lobo, A.C. Silva, Double optimization of rivastigmine-loaded nanostructured lipid carriers (NLC) for nose-to-brain delivery using the quality by design (QbD) approach: Formulation variables and instrumental parameters, Pharmaceutics. 12 (2020) 1–27. https://doi.org/10.3390/pharmaceutics12070599.
[132] Y. Xiang, Y. Long, Q. Yang, C. Zheng, M. Cui, Z. Ci, X. Lv, N. Li, R. Zhang, Pharmacokinetics, pharmacodynamics and toxicity of Baicalin liposome on cerebral ischemia reperfusion injury rats via intranasal administration, Brain Res. 1726 (2020) 146503. https://doi.org/10.1016/j.brainres.2019.146503.
[133] R.R. Padalkar, A.R. Madgulkar, M.R. Bhalekar, Brain Targeted Delivery of Rizatriptan using Glutathione Conjugated Liposomes through Transmucosal Nasal Route, Int. J. Pharm. Investig. 10 (2020) 344–350. https://doi.org/10.5530/ijpi.2020.3.61.
[134] H.K. Dhaliwal, Y. Fan, J. Kim, M.M. Amiji, Intranasal Delivery and Transfection of mRNA Therapeutics in the Brain Using Cationic Liposomes, Mol. Pharm. 17 (2020) 1996–2005. https://doi.org/10.1021/acs.molpharmaceut.0c00170.
[135] K.M. Hosny, Nanosized cubosomal thermogelling dispersion loaded with saquinavir mesylate to improve its bioavailability: Preparation, optimization, in vitro and in vivo evaluation, Int. J. Nanomedicine. 15 (2020) 5113–5129. https://doi.org/10.2147/IJN.S261855.
[136] M.Z. Ahmed, U.A. Khan, A. Haye, N.B. Agarwal, N.A. Alhakamy, H.A. Alhadrami, M.H. Warsi, G.K. Jain, Liquid crystalline nanoparticles for nasal delivery of rosuvastatin: Implications on therapeutic efficacy in management of epilepsy, Pharmaceuticals. 13 (2020) 1–15. https://doi.org/10.3390/ph13110356.
[137] K. Inthavong, Z.F. Tian, J.Y. Tu, W. Yang, C. Xue, Optimising nasal spray parameters for efficient drug delivery using computational fluid dynamics, Comput. Biol. Med. 38 (2008) 713–726. https://doi.org/10.1016/j.compbiomed.2008.03.008.
[138] K. Inthavong, Q. Ge, C.M.K.K. Se, W. Yang, J.Y. Tu, Simulation of sprayed particle deposition in a human nasal cavity including a nasal spray device, J. Aerosol Sci. 42 (2011) 100–113. https://doi.org/10.1016/j.jaerosci.2010.11.008.
[139] X. Tong, J. Dong, Y. Shang, K. Inthavong, J. Tu, Effects of nasal drug delivery device and its orientation on sprayed particle deposition in a realistic human nasal cavity, Comput. Biol. Med. 77 (2016) 40–48. https://doi.org/10.1016/j.compbiomed.2016.08.002.
[140] R.T. Steipel, M.D. Gallovic, C.J. Batty, E.M. Bachelder, K.M. Ainslie, Electrospray for generation of drug delivery and vaccine particles applied in vitro and in vivo, Mater. Sci. Eng. C. 105 (2019) 110070. https://doi.org/10.1016/j.msec.2019.110070.

[141] F. Sultan, E. Allaf-Akbari, N. Ashgriz, Effects of a Coflowing Air on the Characteristics of an Electrospray, Aerosol Sci. Eng. 4 (2020) 210–218. https://doi.org/10.1007/s41810-020-00068-0.
[142] D.O. Frank, J.S. Kimbell, S. Pawar, J.S. Rhee, Effects of anatomy and particle size on nasal sprays and nebulizers, Otolaryngol. - Head Neck Surg. 146 (2012) 313–319. https://doi.org/10.1177/0194599811427519.
[143] L. Zhang, J. Huang, T. Si, R.X. Xu, Coaxial electrospray of microparticles and nanoparticles for biomedical applications, Expert Rev. Med. Devices. 9 (2012) 595–612. https://doi.org/10.1586/erd.12.58.
[144] J.D. Ehrick, S.A. Shah, C. Shaw, V.S. Kulkarni, I. Coowanitwong, S. De, J.D. Suman, Considerations for the Development of Nasal Dosage Forms, in: 2013: pp. 99–144. https://doi.org/10.1007/978-1-4614-7978-9_5.
[145] T. Sullivan, Novel advances in rapid manufacturing, deployment, and delivery of intranasally administered drugs and biologics, ONdrugDelivery. (2011) 31–34. file:///home/clement/Téléchargements/OnDrugDeliveryAPR2011.pdf.
[146] J. Xi, Z. Wang, D. Nevorski, T. White, Y. Zhou, Nasal and Olfactory Deposition with Normal and Bidirectional Intranasal Delivery Techniques: In Vitro Tests and Numerical Simulations, J. Aerosol Med. Pulm. Drug Deliv. 30 (2017) 118–131. https://doi.org/10.1089/jamp.2016.1295.
[147] O. Misik, M. Maly, O. Cejpek, F. Lizal, Characterization of Aerosol Nebulized by Aerogen Solo Mesh Nebulizer, MATEC Web Conf. 328 (2020) 01006. https://doi.org/10.1051/matecconf/202032801006.
[148] A. Claxton, L.D. Baker, A. Hanson, E.H. Trittschuh, B. Cholerton, A. Morgan, M. Callaghan, M. Arbuckle, C. Behl, S. Craft, Long-Acting Intranasal Insulin Detemir Improves Cognition for Adults with Mild Cognitive Impairment or Early-Stage Alzheimer's Disease Dementia, J. Alzheimer's Dis. 44 (2015) 897–906. https://doi.org/10.3233/JAD-141791.
[149] J. Hoekman, S. Ray, S.K. Aurora, S.B. Shrewsbury, The Upper Nasal Space—A Novel Delivery Route Ideal for Central Nervous System Drugs, US Neurol. 16 (2020) 25. https://doi.org/10.17925/USN.2020.16.1.25.
[150] A.R. Khan, M. Liu, M.W. Khan, G. Zhai, Progress in brain targeting drug delivery system by nasal route, J. Control. Release. 268 (2017) 364–389. https://doi.org/10.1016/j.jconrel.2017.09.001.
[151] P.G. Djupesland, Nasal drug delivery devices: characteristics and performance in a clinical perspective—a review, Drug Deliv. Transl. Res. 3 (2013) 42–62. https://doi.org/10.1007/s13346-012-0108-9.
[152] S. Khalili, N. Tkachenko, B. Rotenberg, A novel device for delivery of intranasal particulate medication: a pilot study: {Novel} device for nasal particulate delivery, Int. Forum Allergy \& Rhinol. 3 (2013) 905–910. https://doi.org/10.1002/alr.21199.
[153] P.G. Djupesland, A. Skretting, Nasal deposition and clearance in man: Comparison of a bidirectional powder device and a traditional liquid spray pump, J. Aerosol Med. Pulm. Drug Deliv. 25 (2012) 280–289. https://doi.org/10.1089/jamp.2011.0924.
[154] M.Y. Foo, Y.-S.S. Cheng, W.-C.C. Su, M.D. Donovan, The Influence of Spray Properties on Intranasal Deposition, J. Aerosol Med. 20 (2007) 495–508. https://doi.org/10.1089/jam.2007.0638.
[155] M. Kiaee, H. Wachtel, M.L. Noga, A.R. Martin, W.H. Finlay, An idealized geometry that mimics average nasal spray deposition in adults: A computational study, Comput. Biol. Med. 107 (2019) 206–217. https://doi.org/10.1016/j.compbiomed.2019.02.013.
[156] S. Trows, R. Scherließ, Carrier-based dry powder formulation for nasal delivery of vaccines utilizing BSA as model drug, Powder Technol. 292 (2016) 223–231.

https://doi.org/10.1016/j.powtec.2016.01.042.
[157] R.S. Kaye, T.S. Purewal, O.H. Alpar, Development and testing of particulate formulations for the nasal delivery of antibodies, J. Control. Release. 135 (2009) 127–135. https://doi.org/10.1016/j.jconrel.2008.11.009.
[158] T.R. Sosnowski, P. Rapiejko, J. Sova, K. Dobrowolska, Impact of physicochemical properties of nasal spray products on drug deposition and transport in the pediatric nasal cavity model, Int. J. Pharm. 574 (2020) 118911. https://doi.org/10.1016/j.ijpharm.2019.118911.
[159] Y.S. Cheng, T.D. Holmes, J. Gao, R.A. Guilmette, S. Li, Y. Surakitbanharn, C. Rowlings, Characterization of Nasal Spray Pumps and Deposition Pattern in a Replica of the Human Nasal Airway, J. Aerosol Med. 14 (2001) 267–280. https://doi.org/10.1089/08942680152484199.
[160] Mukesh K. Agarwala, Vikram R. Jamalabad, Noshir A. Langrana, Ahmad Safari, Philip J. Whalen and, Stephen C. Danforth, Structural quality of parts processed by fused deposition, Rapid Prototyp. J. 2 (1996) 4–19.
[161] J.P. Kruth, G. Levy, F. Klocke, T.H.C. Childs, Consolidation phenomena in laser and powder-bed based layered manufacturing, CIRP Ann. - Manuf. Technol. 56 (2007) 730–759. https://doi.org/10.1016/j.cirp.2007.10.004.
[162] S. Lungare, J. Bowen, R. Badhan, Development and Evaluation of a Novel Intranasal Spray for the Delivery of Amantadine, J. Pharm. Sci. 105 (2016) 1209–1220. https://doi.org/10.1016/j.xphs.2015.12.016.
[163] S.K. Kim, Y. Na, J.-I. Kim, S.-K. Chung, Patient specific CFD models of nasal airflow: Overview of methods and challenges, J. Biomech. 46 (2013) 299–306. https://doi.org/10.1016/j.jbiomech.2012.11.022.
[164] G. Xiong, J. Zhan, K. Zuo, J. Li, L. Rong, G. Xu, Numerical flow simulation in the post-endoscopic sinus surgery nasal cavity, Med. Biol. Eng. Comput. 46 (2008) 1161–1167. https://doi.org/10.1007/s11517-008-0384-1.
[165] J.Z. Chen, M. Kiaee, A.R. Martin, W.H. Finlay, In vitro assessment of an idealized nose for nasal spray testing: Comparison with regional deposition in realistic nasal replicas, Int. J. Pharm. 582 (2020) 119341. https://doi.org/10.1016/j.ijpharm.2020.119341.
[166] A.A. Gungor, The aerodynamics of the sinonasal interface: the nose takes wing-a paradigm shift for our time, Int. Forum Allergy Rhinol. 3 (2013) 299–306. https://doi.org/10.1002/alr.21105.
[167] J.A. Keeler, A. Patki, C.R. Woodard, D.O. Frank-Ito, A Computational Study of Nasal Spray Deposition Pattern in Four Ethnic Groups, J. Aerosol Med. Pulm. Drug Deliv. 29 (2016) 153–166. https://doi.org/10.1089/jamp.2014.1205.
[168] W. Keustermans, T. Huysmans, B. Schmelzer, J. Sijbers, J.J.J. Dirckx, The effect of nasal shape on the thermal conditioning of inhaled air: Using clinical tomographic data to build a large-scale statistical shape model, Comput. Biol. Med. 117 (2020) 103600. https://doi.org/10.1016/j.compbiomed.2020.103600.
[169] V. Quatela, J. Pearson, Management of the Aging Nose, Facial Plast. Surg. 25 (2009) 215–221. https://doi.org/10.1055/s-0029-1242032.
[170] Y. Liu, M.R. Johnson, E.A. Matida, S. Kherani, J. Marsan, Creation of a standardized geometry of the human nasal cavity, J. Appl. Physiol. 106 (2009) 784–795. https://doi.org/10.1152/japplphysiol.90376.2008.
[171] F. Calignano, D. Manfredi, E.P. Ambrosio, S. Biamino, M. Lombardi, E. Atzeni, A. Salmi, P. Minetola, L. Iuliano, P. Fino, Overview on Additive Manufacturing Technologies, Proc. IEEE. 105 (2017) 593–612. https://doi.org/10.1109/JPROC.2016.2625098.

[172] A. Goyanes, U. Det-Amornrat, J. Wang, A.W. Basit, S. Gaisford, 3D scanning and 3D printing as innovative technologies for fabricating personalized topical drug delivery systems, J. Control. Release. 234 (2016) 41–48. https://doi.org/10.1016/j.jconrel.2016.05.034.
[173] J. Goole, K. Amighi, {3D} printing in pharmaceutics: {A} new tool for designing customized drug delivery systems, Int. J. Pharm. 499 (2016) 376–394. https://doi.org/10.1016/j.ijpharm.2015.12.071.
[174] H. Kim, Y. Lin, T.-L.B. Tseng, A review on quality control in additive manufacturing, Rapid Prototyp. J. 24 (2018) 645–669. https://doi.org/10.1108/RPJ-03-2017-0048.
[175] G.B. Kim, S. Lee, H. Kim, D.H. Yang, Y.-H. Kim, Y.S. Kyung, C.-S. Kim, S.H. Choi, B.J. Kim, H. Ha, S.U. Kwon, N. Kim, Three-Dimensional Printing: Basic Principles and Applications in Medicine and Radiology, Korean J. Radiol. 17 (2016) 182. https://doi.org/10.3348/kjr.2016.17.2.182.
[176] R. Löffler, M. Koch, Innovative Extruder Concept for Fast and Efficient Additive Manufacturing, IFAC-PapersOnLine. 52 (2019) 242–247. https://doi.org/10.1016/j.ifacol.2019.10.071.
[177] A. El Moumen, M. Tarfaoui, K. Lafdi, Modelling of the temperature and residual stress fields during 3D printing of polymer composites, Int. J. Adv. Manuf. Technol. 104 (2019) 1661–1676. https://doi.org/10.1007/s00170-019-03965-y.
[178] Z. Geng, B. Bidanda, Geometric precision analysis for Additive Manufacturing processes: A comparative study, Precis. Eng. 69 (2021) 68–76. https://doi.org/10.1016/j.precisioneng.2020.12.022.
[179] S.C. Ligon, R. Liska, J. Stampfl, M. Gurr, R. Mülhaupt, Polymers for 3D Printing and Customized Additive Manufacturing, Chem. Rev. 117 (2017) 10212–10290. https://doi.org/10.1021/acs.chemrev.7b00074.
[180] K.S. Erokhin, E.G. Gordeev, V.P. Ananikov, Revealing interactions of layered polymeric materials at solid-liquid interface for building solvent compatibility charts for 3D printing applications, Sci. Rep. 9 (2019). https://doi.org/10.1038/s41598-019-56350-w.
[181] E.G. Gordeev, A.S. Galushko, V.P. Ananikov, Improvement of quality of 3D printed objects by elimination of microscopic structural defects in fused deposition modeling, PLoS One. 13 (2018). https://doi.org/10.1371/journal.pone.0198370.
[182] M. Vaezi, S. Chianrabutra, B. Mellor, S. Yang, Multiple material additive manufacturing – Part 1: a review, Virtual Phys. Prototyp. 8 (2013) 19–50. https://doi.org/10.1080/17452759.2013.778175.
[183] J.T. Kelly, B. Asgharian, J.S. Kimbell, B.A. Wong, Particle Deposition in Human Nasal Airway Replicas Manufactured by Different Methods. Part I: Inertial Regime Particles, Aerosol Sci. Technol. 38 (2004) 1072–1079. https://doi.org/10.1080/027868290883360.
[184] S. Mukai, E. Mukai, J.A. Santos-Junior, J.A. Shibli, M. Faveri, G. Giro, Assessment of the reproducibility and precision of milling and 3D printing surgical guides, BMC Oral Health. 21 (2021) 1. https://doi.org/10.1186/s12903-020-01362-6.
[185] F. Kotz, P. Risch, D. Helmer, B.E. Rapp, Highly fluorinated methacrylates for optical 3D printing of microfluidic devices, Micromachines. 9 (2018). https://doi.org/10.3390/mi9030115.
[186] K. Kletetschka, J.D. Rimstidt, T.E. Long, F.M. Michel, Suitability of 3D-Printed devices for low-temperature geochemical experiments, Appl. Geochemistry. 98 (2018) 121–126. https://doi.org/10.1016/j.apgeochem.2018.08.012.
[187] K. Zhao, K. Kim, J.R. Craig, J.N. Palmer, Using 3D printed sinonasal models to visualize and optimize personalized sinonasal sinus irrigation strategies, Rhinol. J.

(2020) 0. https://doi.org/10.4193/Rhin19.314.
[188] C.R. Hatz, B. Msallem, S. Aghlmandi, P. Brantner, F.M. Thieringer, Can an entry-level 3D printer create high-quality anatomical models? Accuracy assessment of mandibular models printed by a desktop 3D printer and a professional device, Int. J. Oral Maxillofac. Surg. 49 (2020) 143–148. https://doi.org/10.1016/j.ijom.2019.03.962.
[189] S. Chandra, Trends in Selective Laser Sintering in Biomedical Engineering, Int. J. Emerg. Trends Eng. Res. 8 (2020) 54–59. https://doi.org/10.30534/ijeter/2020/10812020.
[190] C. Gayer, J. Ritter, M. Bullemer, S. Grom, L. Jauer, W. Meiners, A. Pfister, F. Reinauer, M. Vučak, K. Wissenbach, H. Fischer, R. Poprawe, J.H. Schleifenbaum, Development of a solvent-free polylactide/calcium carbonate composite for selective laser sintering of bone tissue engineering scaffolds, Mater. Sci. Eng. C. 101 (2019) 660–673. https://doi.org/10.1016/j.msec.2019.03.101.
[191] C.G.Y. Ngan, C.D. O'Connell, R. Blanchard, M. Boyd-Moss, R.J. Williams, J. Bourke, A. Quigley, P. McKelvie, R.M.I. Kapsa, P.F.M. Choong, Optimising the biocompatibility of 3D printed photopolymer constructs in vitro and in vivo, Biomed. Mater. 14 (2019) 35007. https://doi.org/10.1088/1748-605X/ab09c4.
[192] S.-J. Jin, D.-Y. Kim, J.-H. Kim, W.-C. Kim, Accuracy of Dental Replica Models Using Photopolymer Materials in Additive Manufacturing: In Vitro Three-Dimensional Evaluation, J. Prosthodont. 28 (2019) e557–e562. https://doi.org/10.1111/jopr.12928.
[193] R. Bansil, B.S. Turner, The biology of mucus: Composition, synthesis and organization, Adv. Drug Deliv. Rev. 124 (2018) 3–15. https://doi.org/10.1016/j.addr.2017.09.023.
[194] J.D. Schroeter, G.J.M. Garcia, J.S. Kimbell, Effects of surface smoothness on inertial particle deposition in human nasal models, J. Aerosol Sci. 42 (2011) 52–63. https://doi.org/10.1016/j.jaerosci.2010.11.002.
[195] J.Z. Chen, I.M. Katz, M. Pichelin, K. Zhu, G. Caillibotte, M.L. Noga, W.H. Finlay, A.R. Martin, Comparison of pulsed versus continuous oxygen delivery using realistic adult nasal airway replicas, Int. J. Chron. Obstruct. Pulmon. Dis. Volume 12 (2017) 2559–2571. https://doi.org/10.2147/COPD.S141976.
[196] A. Altundag, D. Temirbekov, C. Haci, D. Yildirim, M. Cayonu, Olfactory Cleft Width and Volume: Possible Risk Factors for Postinfectious Olfactory Dysfunction, Laryngoscope. 131 (2021) 5–9. https://doi.org/10.1002/lary.28524.
[197] G.A. Khalid, H. Bakhtiarydavijani, W.R. Whittington, R. Prabhu, M.D. Jones, Material response characterization of three poly jet printed materials used in a high fidelity human infant skull, Mater. Today Proc. 20 (2020) 408–413. https://doi.org/10.1016/j.matpr.2019.09.156.
[198] E.A. Clark, M.R. Alexander, D.J. Irvine, C.J. Roberts, M.J. Wallace, S. Sharpe, J. Yoo, R.J.M. Hague, C.J. Tuck, R.D. Wildman, 3D printing of tablets using inkjet with UV photoinitiation, Int. J. Pharm. 529 (2017) 523–530. https://doi.org/10.1016/j.ijpharm.2017.06.085.
[199] Z. Muwaffak, A. Goyanes, V. Clark, A.W. Basit, S.T. Hilton, S. Gaisford, Patient-specific 3D scanned and 3D printed antimicrobial polycaprolactone wound dressings, Int. J. Pharm. 527 (2017) 161–170. https://doi.org/10.1016/j.ijpharm.2017.04.077.
[200] S.A. Khaled, M.R. Alexander, R.D. Wildman, M.J. Wallace, S. Sharpe, J. Yoo, C.J. Roberts, 3D extrusion printing of high drug loading immediate release paracetamol tablets, Int. J. Pharm. 538 (2018) 223–230. https://doi.org/10.1016/j.ijpharm.2018.01.024.
[201] S. Le Guellec, D. Le Pennec, S. Gatier, L. Leclerc, M. Cabrera, J. Pourchez, P. Diot, G. Reychler, L. Pitance, M. Durand, F. Jamar, L. Vecellio, Validation of anatomical

models to study aerosol deposition in human nasal cavities, Pharm. Res. 31 (2014) 228–237. https://doi.org/10.1007/s11095-013-1157-6.
[202] T. Sartoretti, M. Mannil, S. Biendl, J.M. Froehlich, H. Alkadhi, M. Zadory, In vitro qualitative and quantitative CT assessment of iodinated aerosol nasal deposition using a 3D-printed nasal replica, Eur. Radiol. Exp. 3 (2019) 32. https://doi.org/10.1186/s41747-019-0113-6.
[203] J. Xi, T. Demski, Y. Fallatah, K. Mcdonnell, SM Gr up SM Journal of Biomedical Engineering Experimental Test of Olfactory Deposition of Charged Particles under Electric Field Guidance and Bi- directional Breathing Conditions, 2 (2016) 1–7.
[204] S. Häußermann, A.G. Bailey, M.R. Bailey, G. Etherington, M. Youngman, The influence of breathing patterns on particle deposition in a nasal replicate cast, J. Aerosol Sci. 33 (2002) 923–933. https://doi.org/10.1016/S0021-8502(02)00044-7.
[205] V. Kundoor, R.N. Dalby, Effect of formulation- and administration-related variables on deposition pattern of nasal spray pumps evaluated using a nasal cast, Pharm. Res. 28 (2011) 1895–1904. https://doi.org/10.1007/s11095-011-0417-6.
[206] D.-W.W. Kim, S.-K.K. Chung, Y. Na, Numerical study on the air conditioning characteristics of the human nasal cavity, Comput. Biol. Med. 86 (2017) 18–30. https://doi.org/10.1016/j.compbiomed.2017.04.018.
[207] P.G. Djupesland, J.C. Messina, R.A. Mahmoud, Role of nasal casts for in vitro evaluation of nasal drug delivery and quantitative evaluation of various nasal casts, Ther. Deliv. 11 (2020) 485–495. https://doi.org/10.4155/tde-2020-0054.
[208] L. Grunberg, A.H. Nissan, Mixture law for viscosity [21], Nature. 164 (1949) 799–800. https://doi.org/10.1038/164799b0.
[209] O. Lafforgue, I. Seyssiecq, S. Poncet, J. Favier, Rheological properties of synthetic mucus for airway clearance, J. Biomed. Mater. Res. - Part A. 106 (2018) 386–396. https://doi.org/10.1002/jbm.a.36251.
[210] R.A. Cone, Barrier properties of mucus, Adv. Drug Deliv. Rev. 61 (2009) 75–85. https://doi.org/10.1016/j.addr.2008.09.008.
[211] J.M. Zham, M. King, C. Duvivier, D. Pierrot, S. Girod, E. Puchelle, J.M. Zahm, M. King, C. Duvivier, D. Pierrot, S. Girod, E. Puchelle, Role of simulated repetitive coughing in mucus clearance, Eur. Respir. 4 (1991) 311–315. https://erj.ersjournals.com/content/4/3/311.
[212] O. Lafforgue, I. Seyssiecq, S. Poncet, J. Favier, Rheological properties of synthetic mucus for airway clearance: Rheological Properties of Synthetic Mucus, J. Biomed. Mater. Res. Part A. 106 (2018) 386–396. https://doi.org/10.1002/jbm.a.36251.
[213] E. Puchelle, J.M. Zahm, D. Quemada, Rheological properties controlling mucociliary frequency and respiratory mucus transport, Biorheology. 24 (1987) 557–563. https://doi.org/10.3233/BIR-1987-24606.
[214] A.-I.I. Bunea, M.H. Jakobsen, E. Engay, A.R. Bañas, J. Glückstad, Optimization of 3D-printed microstructures for investigating the properties of the mucus biobarrier, Micro Nano Eng. 2 (2019) 41–47. https://doi.org/10.1016/j.mne.2018.12.004.
[215] M. Gross, X. Zhao, V. Mascarenhas, Z. Wen, Effects of the surface physico-chemical properties and the surface textures on the initial colonization and the attached growth in algal biofilm, Biotechnol. Biofuels. 9 (2016) 1–14. https://doi.org/10.1186/s13068-016-0451-z.